

8-2020

Histological and functional characterization of cervical spinal cord injury after graded contusion

Chrystine Gallegos

Follow this and additional works at: https://digitalcommons.library.tmc.edu/utgsbs_dissertations



Part of the [Medicine and Health Sciences Commons](#)

Recommended Citation

Gallegos, Chrystine, "Histological and functional characterization of cervical spinal cord injury after graded contusion" (2020). *The University of Texas MD Anderson Cancer Center UTHealth Graduate School of Biomedical Sciences Dissertations and Theses (Open Access)*. 1037.

https://digitalcommons.library.tmc.edu/utgsbs_dissertations/1037

This Thesis (MS) is brought to you for free and open access by the The University of Texas MD Anderson Cancer Center UTHealth Graduate School of Biomedical Sciences at DigitalCommons@TMC. It has been accepted for inclusion in The University of Texas MD Anderson Cancer Center UTHealth Graduate School of Biomedical Sciences Dissertations and Theses (Open Access) by an authorized administrator of DigitalCommons@TMC. For more information, please contact digitalcommons@library.tmc.edu.

HISTOLOGICAL AND FUNCTIONAL CHARACTERIZATION OF CERVICAL SPINAL CORD INJURY AFTER
GRADED CONTUSION

by

Chrystine Marie Gallegos, B.A.

APPROVED:



Qi Lin Cao, M.D.
Advisory Professor



Radbod Darabi, Ph.D.



Ying Liu, M.D., Ph.D.



Laura Smith-Callahan, Ph.D.



Qingchun Tong, Ph.D.



Jiaqian Wu, Ph.D.

APPROVED:

Dean, The University of Texas
MD Anderson Cancer Center UTHealth Graduate School of Biomedical Sciences

HISTOLOGICAL AND FUNCTIONAL CHARACTERIZATION OF CERVICAL SPINAL CORD INJURY AFTER
GRADED CONTUSION

A

THESIS

Presented to the Faculty of

The University of Texas

MD Anderson Cancer Center UTHealth

Graduate School of Biomedical Sciences

in Partial Fulfillment

of the Requirements for the Degree of

MASTER OF SCIENCE

by

Chrystine Marie Gallegos, B.A.

Houston, Texas

August, 2020

For Kate and Dr. Gustin

ACKNOWLEDGEMENTS

Before I jump into the individual “thank you’s”, I would like to first take a moment to thank every person who has supported me, this project, and my dreams over the past two years. I could not have done this without you.

I would first like to thank my labmates, Yiyan and Matthew, for their time, support, and patience. Without you, this project would not have been possible, so thank you for your help. I would like to thank our collaborators in the Liu lab, especially Haipeng for designing the virus constructs. Mei and Jorge, thank you for all the patient guidance and spending time helping me with any of my microscope/technological difficulties. I would also like to thank all of my fellow lab colleagues on the 6th floor. Jose and Varada, thank you for answering my endless GSBS questions, your advice but most importantly support. Henry and Sean, thank you for the laughs, the help, and providing calming words when things got a little wild. Eyad and Xizi, thank you for helping me become a better scientist and writer, explaining answers to all my questions, and just being great.

I would like to thank my committee for engaging meetings, support, and guidance as I’ve learned over the past two years. I would also like to thank the GSBS and UTHealth community for their constant support. A huge thank you to all of the professors that have helped me over the past couple of years. Dr. Magnotti, thank you for answering my continual emails and your endless patience and enthusiasm. I would like to thank the vet staff and CLAMC for their animal care, and especially Chris Janssen. Thank you for teaching me about animal training – you have helped shape me as a scientist.

To my friends and family, you’ve been my lifeline. A humongous thank you to my mom, dad, grandparents, and all my other family members. To my friends, your support has meant more than you know, especially when the going got tough. Zoe, your support (and donuts) helped me through some really tough times. Kate, you changed my life, and you know why. To the new and fantastic

people in my life, Tara and Max, thank you for all the time you've spent helping me, your endless patience, and your unwavering support, it's meant the world to me. An additional thank you to Dr. Gustin for your mentorship over the past seven years and teaching me how to see science and the world from a glass half full perspective. I wouldn't be where I am today without your help back when I was just a freshman.

And very importantly, I would like to thank my mentor, Dr. Cao, for his unending support and patience. Thank you for being there for me during some of my most formative years and guiding me to become the scientist I am today. Thank you for teaching me how to think critically, how to think about science, and how to communicate my ideas. Thank you for reigning in my writing to the actual topics I was supposed to cover, and for teaching me how to tell my story. Most importantly, thank you for accepting me as a student and for accepting all of my successes and failures. Thank you for letting me explore my ideas and always, always approaching science with excitement and an attitude to see what happens. I have learned an enormous amount from you and am incredibly grateful.

HISTOLOGICAL AND FUNCTIONAL CHARACTERIZATION OF CERVICAL SPINAL CORD INJURY AFTER GRADED CONTUSION

by

Chrystine Marie Gallegos, B.A.

Advisory Professor: Qi Lin Cao, M.D.

Most spinal cord injuries (SCIs) are cervical contusions and result in deficits for both locomotion and reaching and grasping functions. Previous studies have characterized histological and functional deficits in locomotion using primarily thoracic contusions, but most patients have cervical injuries. Damage to descending long spinal tracts (dLSTs) is one well-established cause of functional loss after SCI and has been explored in laceration and transection models, but these are not clinically relevant. In this study, I will explore the histological and functional deficits after graded cervical hemicontusion SCI and examine the potential contribution of different histological deficits to forelimb function after injury. B6 mice received a clinically relevant cervical hemicontusion graded at either 50, 70, or 90 kDyne force and were then tested weekly in complex horizontal ladder (cHL), rotarod, grooming, and either pellet reaching or pasta handling. Our results showed greater injury severity significantly increased missteps in cHL, reduced stepping time in rotarod, and decreased grooming ability. Histological analyses revealed that injury severity significantly increased the injury size by fibronectin-immunoreactivity (IR) and gray matter loss by MAP2-IR. There was a significant correlation between lesion size and gray matter loss and injury severity. Correlations between histology and behavior outcomes showed a significant correlation between the percentage of missteps in cHL, injury severity, and lesion size. Additionally, both rotarod score and grooming score correlated with injury severity, lesion size, and gray matter loss. This study characterizes a clinically relevant injury model, shows that graded cervical hemicontusions result in degrees of functional and anatomical loss, and serves as a

baseline to aid future studies in identifying therapeutic targets to promote functional recovery after cervical SCI and improve the quality of life for patients with SCI.

Table of Contents

APPROVAL PAGE.....	i
TITLE PAGE.....	ii
DEDICATION.....	iii
ACKNOWLEDGMENTS.....	iv-v
ABSTRACT.....	vi-vii
LIST OF ILLUSTRATIONS.....	xi
LIST OF TABLES	xii
ABBREVIATIONS.....	xiii
Chapter 1 – INTRODUCTION.....	1
1.1 – SCI Prevalence	1
1.2 Animal SCI Models.....	2
1.3 – SCI Pathophysiology	4
1.4 – Spinal Tracts.....	5
1.5 – Aims and Hypothesis	7
CHAPTER 2 – MATERIALS AND METHODS.....	9
2.1. Spinal Cord Contusion Injury	10
2.2. Behavioral Assessments	11
2.2.1. Forepaw Assessments	11
2.2.2. Locomotor Assessments.....	14
2.3. Anterograde Tracing for descending Long Spinal Tracts.....	17

2.4. Retrograde tracing by Cholera Toxin B.....	18
2.5. Immunohistochemistry	18
2.4. Histological Analysis	22
2.4.1. Quantification of Injury Size – Fibronectin	22
2.4.2. Quantification of Gray matter Loss – MAP2.....	22
2.4.3. Quantification of descending Propriospinal Spinal Tracts by CTB retrograded tracing.	23
2.5. Statistical Analysis	24
2.5.1. Behavioral Statistics.....	24
2.5.2. IHC Statistics	24
2.5.3. Correlation plots.....	24
Chapter 3 – RESULTS	26
Increasing the severity of SCI contusion results in more missteps in complex horizontal ladder ...	26
Contusion severity reduces time in rotarod score	28
Grooming score reduced in all injury severity groups after unilateral contusion.....	30
The effect of graded SCI on forelimb function in pasta handling and single pellet reaching	32
Overview of histological changes after graded unilateral cervical contusion.....	33
Injury size by fibronectin is significantly greater in 70 and 90 kD contusion SCIs compared to 50 kD	35
Gray matter loss significantly increases after cervical contusion SCI	37
The propriospinal tracts after graded SCI by CTB retrograde tracing.	39
Correlations between histology analysis and functional performance.....	48

Chapter 4 – DISCUSSION	53
Clinically-relevant cervical hemicontusion graded model	53
Functional implications of behavioral tests after graded cervical SCI	55
Histology deficits after graded SCI	58
The relationship between histology and functional deficits	59
Potential roles of descending spinal tracts after cervical SCI.....	61
Future directions and Conclusion.....	62
BIBLIOGRAPHY.....	63
VITA	73

LIST OF ILLUSTRATIONS

Figure 1. Broad overview of spinal interneurons.

Figure 2. Experimental timeline.

Figure 3. Clinically relevant injury model.

Figure 4. Increased missteps in the complex horizontal ladder after graded contusion.

Figure 5. Graded contusion SCI impaired rotarod performance.

Figure 6. Deficits in grooming score after graded cervical SCI.

Figure 7. Overview of the histological effects of cervical hemicontusion.

Figure 8. Injury size by fibronectin.

Figure 9. Gray matter loss by MAP2.

Figure 10. Validation of spinal CTB retrograde tracing in uninjured control animals.

Figure 11. Validation of spinal CTB retrograde tracing in grade SCI animals.

Figure 12. Rostral cross-sections of spinal descending long tracts by anterograde tracing.

Figure 13. Longitudinal sections of spinal descending tracts by anterograde tracing.

Figure 14. Relationships between histology and complex horizontal ladder.

Figure 15. Relationships between histology and rotarod.

Figure 16. Relationships between histology and grooming.

LIST OF TABLES

Table 1. Anterograde tracing injections.

Table 2. Immunohistochemical antibodies.

ABBREVIATIONS

Cholera Toxin subunit B (CTB)

Complex Horizontal Ladder (cHL)

Corticospinal Neurons (CSN)

Corticospinal Tract (CST)

Descending Long Spinal Tract (dLST)

Descending Propriospinal Tract (dPST)

Kilodyne (kD)

Microtubule Associated Protein 2 (MAP2)

National Spinal Cord Injury Statistical Center (NSCISC)

Post-Injury (PI)

Reticulospinal Tract (RtST)

Rubrospinal Tract (RST)

Spinal Cord Injury (SCI)

Chapter 1 – INTRODUCTION

1.1 – SCI Prevalence

Spinal cord injuries (SCI) can dramatically change lives in less than one second, leaving patients with permanent disabilities due to lasting motor and sensory functional loss. SCIs are devastating assaults, and happen when the vertebrae housing the spinal cord are damaged, typically due to automotive accidents, falls, violent crimes, or recreational sporting accidents (Singh et al., 2014; Armour et al., 2016; Center, 2019; Loy and Bareyre, 2019). According to the National Spinal Cord Injury Statistical Center (NSCISC), there are an estimated 291,000 individuals living in the United States currently with SCI and approximately 17,730 new SCI cases annually (Center, 2019). Around 80% of SCIs occur in men and 20% in women, and while the average age at injury is about 35 years old, the most common age is about 19 years old (Center., 2019). SCIs can occur by contusion, compression, laceration, dislocation, or distraction mechanisms (Ko, 2019), but contusion and compression injuries are the most common forms of SCI in humans (DeVivo and Chen, 2011; Cheriyan et al., 2014; Warren et al., 2019). SCIs are classified based on the neurological level and severity of injury, and 54.5% of SCIs occur at the cervical level while 34.8% occur at thoracic, 10.2% at lumbar, and <0.5% at sacral SCIs (Center., 2019). Correspondingly, patients with quadriplegia make up 52.4% of individuals with SCI while 43.5% of patients have a paraplegic status; less than one percent of patients recover after SCI (Center., 2019). These demographics demonstrate the prevalence of cervical SCI and quadriplegia clinically and emphasize the importance of cervical SCI research.

The top priorities for individuals with SCI are improving or regaining mobility, bowel and bladder control, sexual function, and pain management (Simpson et al., 2012; Lo et al., 2016). However, while motor function is a top priority in general, individuals with quadriplegia rank hand and arm function as a top priority in contrast to individuals with paraplegia ranking general mobility as a top priority (Simpson et al., 2012; Lo et al., 2016). Every day, humans perform innumerable tasks

requiring reaching and grasping capabilities. Correspondingly, regaining hand and forearm function is one of the top priorities for quadriplegic patients as recovering these functions even partially would greatly improve their quality of life (Lo et al., 2016).

1.2 Animal SCI Models

Animal studies are used to explore the pathophysiological changes after different mechanisms of SCI and the effects of therapeutic interventions. Rodents are the animal model of choice, comprising 88.4% of SCI models, with rats (72.4%) used most overall and mice (16%) the second most commonly used species (Sharif-Alhoseini et al., 2017). Recently, emphasis on mouse SCI models is increasing as transgenic options and viral targeting offer more experimental manipulability (Cheriyian et al., 2014; Flynn et al., 2017; Atasoy and Sternson, 2018; Noristani et al., 2018; Nishi et al., 2020). More than half of SCIs occur at the cervical level in patients (Center., 2019), but approximately 81% SCI models use thoracic injuries (Sharif-Alhoseini et al., 2017). Common injury mechanisms include contusion (41%), transection (32.5%), and compression (19.4%) (Sharif-Alhoseini et al., 2017). More research is critically needed using clinically relevant cervical SCI models such as contusion injury.

Lacerations account for 32.5% of SCI models, and cervical laceration injuries, including dorsal hemisection and dorsal column transection (Schrimsher and Reier, 1993; Onifer et al., 2005; Lewandowski and Steward, 2014; Kumamaru et al., 2019), lateral hemisection (Anderson et al., 2004; Anderson et al., 2005; Khaing et al., 2012), dorsal quadrant transection (Houle et al., 2006), or specific tract injuries (Fink and Cafferty, 2016) by, have been widely used (Geissler et al., 2013; Sharif-Alhoseini et al., 2017). These injury models often cause a complete lesion in the targeted descending tract(s) and provide very useful information regarding the roles of these tracts in forelimb function (Geissler et al., 2013; Sharif-Alhoseini et al., 2017; Ahmed et al., 2019). Additionally, these injury models are very useful to examine a variety of therapeutic approaches (Anderson et al., 2018) to promote axonal

regeneration and functional recovery after SCI (Fink and Cafferty, 2016). However, these laceration injury models are not clinically relevant since very few SCI patients have laceration injuries and the majority of patients have contusion injuries. Adopted from thoracic contusion injury, the central contusion has been extended to the cervical spinal cord, producing bilateral gray and white matter damages and distinct forelimb functional deficits (Aguilar and Steward, 2010; Guo et al., 2019; Reinhardt et al., 2020). These studies demonstrate the feasibility and reproducibility of bilateral cervical SCI and provide a paradigm of functional deficits for future studies. However, bilateral contusion injury in the cervical region can only be induced in lower cervical segments with high mortality and labor-intensive post-injury animal care (Steward and Willenberg, 2017). To overcome these pitfalls, the unilateral cervical contusion has been developed in both rats and mice (Lee et al., 2012; Streijger et al., 2013). The unilateral contusion injury recapitulates the main pathophysiological changes of contusion SCI and delivers specific forelimb functional deficits on the injury side of the cervical spinal cord but still allows the animal to reach food and water. Unilateral cervical contusion has been increasingly used to evaluate mechanisms of neuronal and axonal response to injury and potential therapeutic approaches for cervical SCI repair (Dai et al., 2011; Lee et al., 2012; Fakhoury, 2015; Mondello et al., 2015; Chhaya et al., 2019; Erskine et al., 2019; Marquardt et al., 2020). Previous work by Streijger et al. 2013 characterized hemicontusions of the cervical spinal cord in C57BL/6 mice with varying dwell times and discovered that the length of time the spinal cord was compressed correlated with reduced performance in behavioral tests and found large amounts of white and gray matter loss using erriochrome cyanine staining (Streijger et al., 2013). This demonstrates that the length of time the tissue is under stress impacts the injury and subsequent motor function, and also shows that SCI results in white and gray matter loss. The specific contributions of white matter and/or gray matter loss to functional deficits are not yet known, although the damage to neurons in the gray matter and severing of axons in the white matter are implicated in the functional deficits after SCI.

How lesions of descending long spinal tracts (dLSTs) and descending propriospinal tracts (dPSTs) contribute to functional deficits is also not yet known for either unilateral or bilateral cervical contusion SCI. Further exploration of how injury severity affects forelimb function as well as their axonal connections would be helpful to predict functional outcomes in recovering SCI patients, but also to develop targeted therapies specific to recovering those missing functions. Models using graded contusion SCI by varying force severities are clinically relevant and could help us understand the functional and anatomical distinctions characterizing between different injury grades.

1.3 – SCI Pathophysiology

Pathophysiology for SCI is comprised of roughly two injuries: primary injury and secondary injury. The primary injury includes the initial mechanical injury to the spinal cord and the damaging events of the acute phase. The initial physical trauma occurs after contusion, compression, laceration, dislocation, or distraction of the spinal cord (Ko, 2019). In the immediate seconds to minutes after injury, the acute phase begins a damaging cascade of events including shearing ascending and descending axons, damaging neuron cell bodies, and breaching the blood-spinal cord-barrier, all of which contribute to the release of factors for necrosis, apoptosis, and alarmin responses (Silva et al., 2014; Tran et al., 2018). The secondary injury overlaps with the primary injury but occurs during the subacute and chronic phase in the minutes, months, and years after injury, and is characterized by chronic inflammation and infiltration by macrophages, monocytes, and leukocytes, upregulation of inhibitory chondroitin sulfate proteoglycans, free radicals, and other damaging reactive molecules (Little, 2006; Silva et al., 2014; Tran et al., 2018). The consequences of both primary and secondary injuries are neuronal loss, demyelination due to the cell death of oligodendrocytes, axonal lesioning, and eventually cavitation and formation of the glial scar in the injury center as well as permanent locomotor and sensory loss below the lesion (Fakhoury, 2015; Tran et al., 2018).

1.4 – Spinal Tracts

The spinal cord is composed of gray matter, which hosts the spinal neurons and their processes, and white matter, which contains ascending and descending axons for afferent and efferent tracts, respectively. Descending long spinal tracts (dLSTs) in the spinal cord originate in different parts of the brain, for example the corticospinal tract (CST) from the motor cortex, the rubrospinal tract (RST) from the red nucleus, and the reticulospinal tract (RtST) from the reticular formation including the raphe nucleus (Haines et al., 2018). Interneurons in the spinal cord can be generalized to two subclasses, local and propriospinal interneurons (Figure 1). Local interneurons project short distances ipsilaterally, contralaterally, or commissurally and aid in reflex and central pattern generation, while propriospinal interneurons project intersegmentally to a vertebral level higher or lower than their cell body and aid in circuitry genesis and coordination (Saliani et al., 2017; Zholudeva et al., 2018; Zavvarian et al., 2020). Propriospinal neurons project tracts that connect between segments but also connect the cervical to lumbar areas. Recent evidence demonstrates that these distant connections by spinal neurons contribute to stability in locomotion and coordination (Ruder et al., 2016). The CST has been implicated in modulating skilled forelimb movement by specific spinal interneurons (Ueno et al., 2018) and a sequential spatiotemporal activation of cortical neurons (Wang et al., 2017). Furthermore, projections by the RtST to commissural interneurons and propriospinal neurons demonstrates that RtST projections play a role in coordination by commissural interneurons (Mitchell et al., 2016).

Axons in the white matter, including the descending and ascending long tracts and propriospinal tracts, are damaged and severed during SCI. Functional loss after SCI has been attributed to the severing of spinal tracts during SCI and the damage to spinal neurons both during necrosis from physical trauma and primary injury as well as apoptosis due to a proliferative inflammatory response (Tran et al., 2018). Injury models using thoracic and lumbosacral SCI models demonstrate that white

matters are significantly damaged after SCI due to the severing and shearing of axons during the primary injury (Cao et al., 2005; Wen et al., 2015; Nishi et al., 2020). Recently, Wang et al. 2017 used a viral targeting system to specifically ablate corticospinal neurons (CSNs) in uninjured mice and cohesively demonstrated CSNs are recruited sequentially to partake in skilled movement circuits and that the CST is involved in reaching and grasping motions (Wang et al., 2017). Using mice without SCI importantly demonstrates the spatiotemporal organization and recruitment pattern of CSNs, but does not answer how, or if, spinal local and propriospinal interneurons contribute to different steps of the reaching and grasping motion.

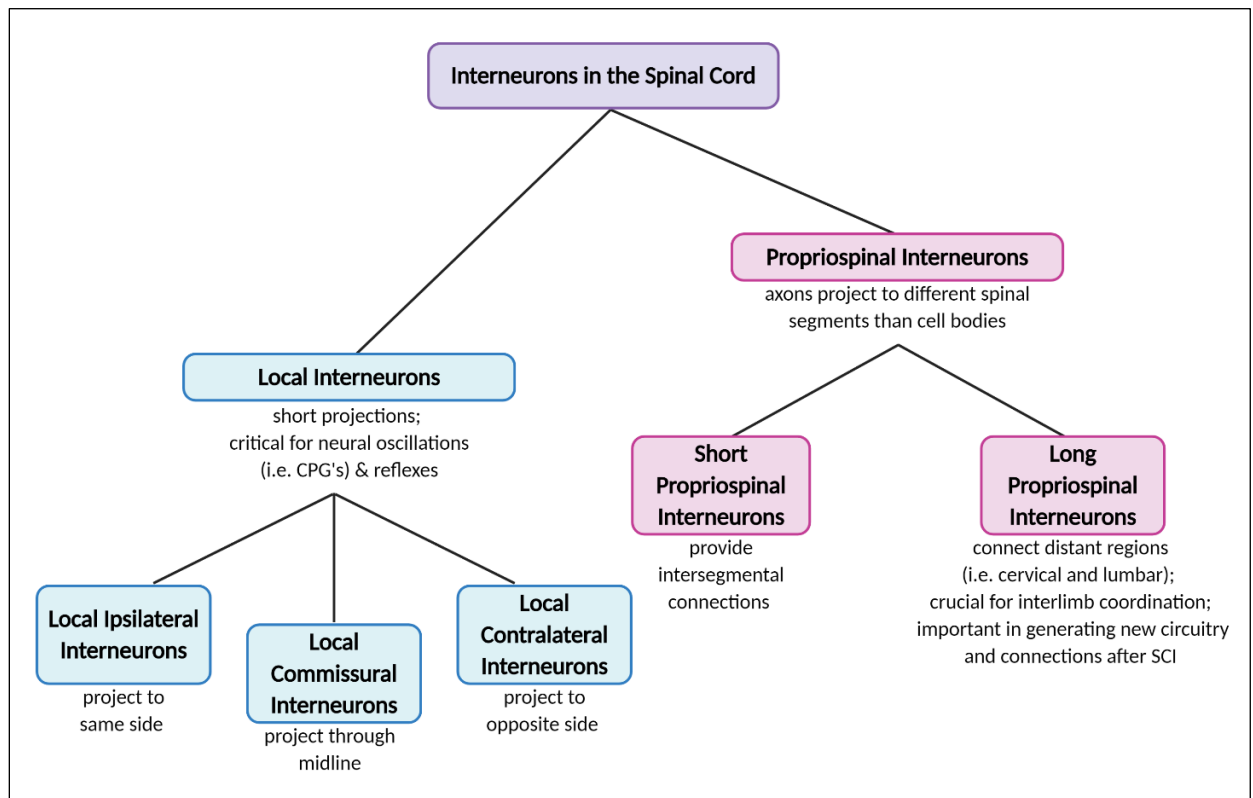


Figure 1 | Interneuron flow chart. Graphical depiction of the different levels of classification for spinal interneurons (Saliani et al., 2017; Zholudeva et al., 2018; Zavvarian et al., 2020). Created with BioRender.com.

1.5 – Aims and Hypothesis

In this study I will characterize the histological and functional deficits after graded cervical SCI, and examine how different histological deficits may contribute to the specific forelimb functional deficits with a focus on the potential contributions of cervical dPSTs in forelimb function after cervical SCI. The long-term goal of this study is to identify the optimized therapeutic targets for the recovery of forelimb function after cervical SCI. Hindlimb deficits after cervical (Dunham et al., 2010; Streijger et al., 2013), thoracic (Cao et al., 2005; Ichiyama et al., 2008), and lumbar (Wen et al., 2015) deficits have been explored, however the cervical spinal cord largely innervates the forelimb, thus more analysis of the forelimb functional deficits after SCI are needed to examine the mechanism of functional loss after cervical SCI. Transection and laceration models offer a clean analysis and have contributed significantly to the SCI field by examining axonal connections, plasticity, and sprouting after injury and during regeneration, but are not clinically relevant. Contusions are the most common mechanism of injury and the cervical region is the most common injured region (Center., 2019), so more research into the anatomy of the spinal cord after contusion is needed to examine potential key players in axonal loss and neuronal death, as well as therapies to promote plasticity and regeneration. Graded SCI models offer an additional advantage because this allows us to sensitively explore degrees of functional loss and anatomical loss between different severities of contusion mechanism.

The roles of descending tracts in forelimb and hindlimb function have been explored, but more research for the contribution of propriospinal tracts to functional deficit after SCI is necessary and could help us identify ways to develop routes around the SCI lesion area and create circuitry detours that could reconnect caudal spinal cord components. The potential of dPST regeneration and plasticity in locomotion recovery remains understudied.

This study is important to examine the roles of dPSTs in forelimb function and functional deficits after cervical SCI. Currently, there are no effective treatments to paralysis after SCI and while

dLSTs have been explored, more work is needed to assess the involvement of dPSTs. This study can help learn and understand mechanisms for these functional deficits and help identify potential therapeutic targets for future studies. Further elucidating which tracts play significant roles – whether cortical or propriospinal – could help us better develop treatments for promoting functional recovery.

In this study, we will examine the contribution of dPSTs in forelimb locomotion deficits after clinically relevant cervical contusion SCI. We hypothesize that cervical dPSTs play an important role in forelimb function and that damage to dPSTs combined with the severing of dLSTs contributes to forelimb functional deficits after cervical SCI. We will test this hypothesis by examining the functional deficits in different injury severities by behavioral assays and by examining different degrees of anatomical damage histologically after graded contusion. The purpose of behavioral assays is to confirm our injury model was effective and repeatable. The purpose of histological analysis is to examine the anatomical details for injury size, gray matter loss, and descending propriospinal neurons which we correlated with functional loss.

We found that different grades of cervical contusion SCI resulted in different degrees of functional loss for the rotarod, complex horizontal ladder, and grooming tests. We concluded that our tests for forelimb specific function by pasta handling and pellet reaching were not effective for assessing graded SCI in mice. Injury size and gray matter loss assessed by fibronectin- and MAP2-IR, respectively, confirmed that our injury model was effective at delivering different injury severities. In this thesis, the following sections will discuss the methods used, the results found, and the significance of our findings and potential future studies.

There currently is no effective treatment for SCI patients. This study will help us understand mechanisms for functional deficits and could aid in identifying therapeutic targets to promote better functional recovery and significantly improve the quality of life for SCI patients.

CHAPTER 2 – MATERIALS AND METHODS

This chapter is based upon: Gallegos C, Carey M, Zheng Y, He X, and Cao QL (2020) Reaching and Grasping Training Improves Functional Recovery After Chronic Cervical Spinal Cord Injury. *Frontiers in Cellular Neuroscience*. Volume 14: Issue 110. DOI: 10.3389/fncel.2020.00110. Portions of the text are granted open-access to the authors from Creative Commons Attribution 4.0 International Public License (CC BY; “Public License”). **Copyright** © 2020 Gallegos, Carey, Zheng, He and Cao.

All animal care, behavioral testing, and surgical interventions were performed in strict accordance to the approval of the Animal Welfare Committee at the University of Texas Health Science Center at Houston. Figure 2 represents an experimental timeline for the animal training, behavioral tests, and surgical procedures.

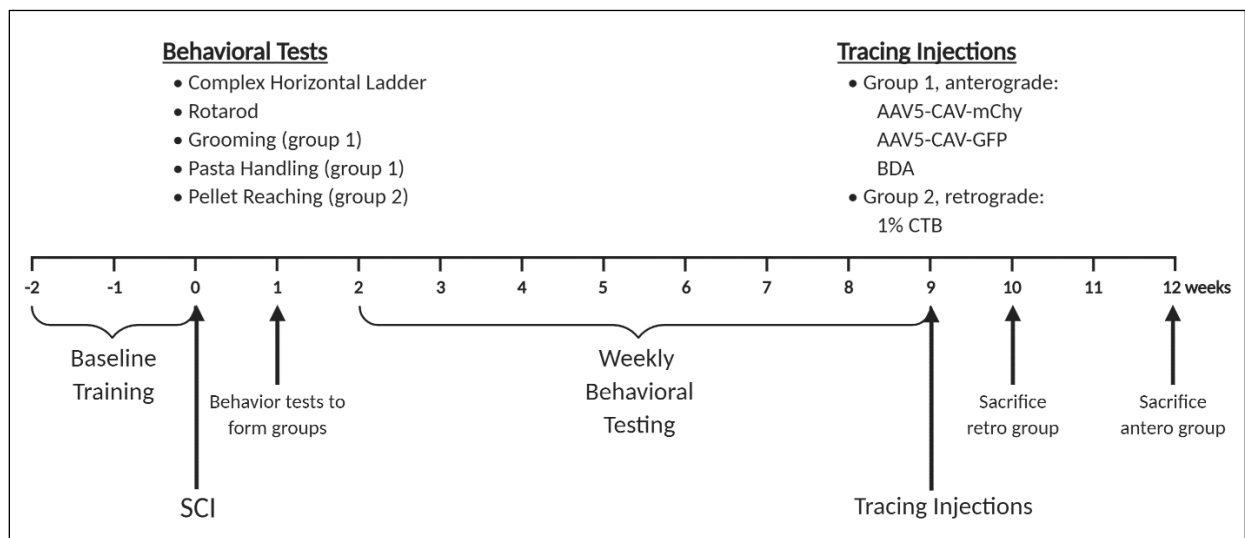


Figure 2 | Experimental timeline of behavioral testing and surgical procedures. Created with BioRender.com.

2.1. Spinal Cord Contusion Injury

The surgical procedures for SCI were performed as previously described (Chen et al., 2013; Fan et al., 2013; Gallegos et al., 2020). Age-matched male and female adult (90-120 days) C57BL/6 [Charles River, Stock no. 000664; body weight, 23.83 ± 2.18 g (female) and 27.94 ± 4.05 g (male)] were used in this study. Three different severities of SCI contusion were performed with 12 mice in each group (total n = 36 mice). Briefly, mice were anesthetized with a mixed solution of ketamine [80 mg/kg, intraperitoneal (ip)] and xylazine (10 mg/kg, ip), and a dorsal laminectomy at the fifth cervical vertebral level (C5) was performed to expose the spinal cord. To prevent lateral torsion as described previously (Lee et al., 2010; Lee et al., 2012), the spinal column was stabilized using steel stabilizers inserted under the transverse processes one vertebra above and below C5 as described in previous contusion models (Hill et al., 2009; Chen et al., 2013; Wu et al., 2017). Mice were then moved to an Infinite Horizons Spinal Cord Impactor (Infinite Horizons LLC, Lexington, Kentucky, US) and carefully positioned below the impactor to receive a unilateral contusive SCI in the preferred paw side as determined by the baseline forelimb behavioral tests (described below in 2.2.1) and then mice were randomly distributed into one of the three injury groups. The software (IH Spinal Cord Impactor v5.0) was set to deliver the appropriate contusion impact force level: mild, 50kD; moderate, 70kD; severe, 90kD (Figure 3). Two mice in each group died during surgery (total mice dead, n = 6). Afterward, the incision was sutured in layers, bacitracin ointment (Qualitest Pharmaceuticals, Huntsville, Alabama, US) was applied to the wound area, 0.1 mL of gentamicin [stock solution 20 mg/ml, subcutaneous (sc); ButlerSchein, Dublin, Ohio, US] was injected, and the animals recovered on soft bedding on a water-circulating heating pad. Mice received a mixed solution of gentamicin antibiotic and buprenorphine analgesic agent (0.05 mg/kg, sc; Reckitt Benckise, Hull, England), once a day for 3 days. Mice were monitored carefully post-operatively, and if mice appeared weakened were given 1-2mL Ringers saline solution (0.03% bacteriostatic saline solution, sc).

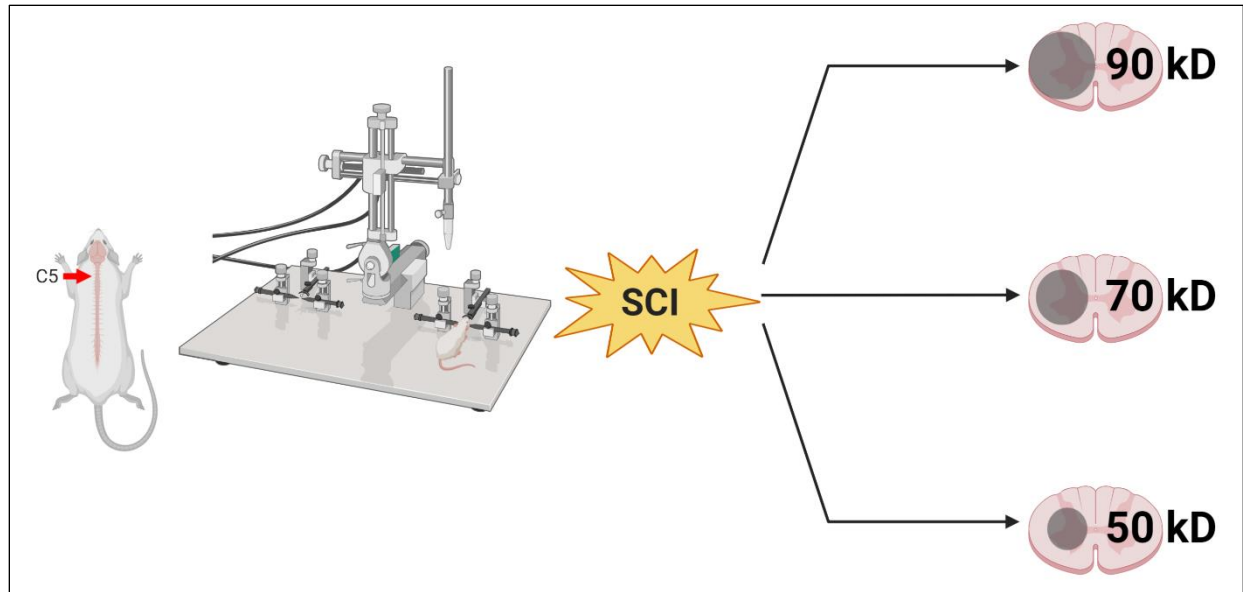


Figure 3 | Illustration of injury model. Mouse (far left) with C5 indicated (red arrow) and representation of IH Impactor injury device. Depiction of group separation with indicated unilateral contusion force levels; 3 groups total, 10 mice per group. Created with Biorender.com.

2.2. Behavioral Assessments

2.2.1. Forepaw Assessments

In the mouse and rat models, cervical SCI affects the forelimbs primarily, although some deficit is observed in the hindlimbs and generally resolves in 1-2 weeks depending on injury severity. As the majority of SCIs occur in the cervical region, we wanted to evaluate the functional deficits observed in the three different injury severity levels – 50, 70, 90kD – over time.

2.2.1.1. Pasta Handling

Forepaw dexterity and reaching and grasping kinematics have been well explored in previous studies (Allred et al., 2008; Tennant et al., 2010; Whishaw et al., 2017). In this study, pasta handling was used to evaluate forepaw function in the mouse after graded SCI over a period of nine weeks. Mice were trained in the pasta handling task with a custom-built enclosure of a mirror floor (20 cm

diameter single plane circle mirror, Hobby Lobby) and 12 cm long x 12 cm wide x 21 cm height matte white foamboard with nonporous coating for cleaning. The front wall was made of clear, thin plexiglass to allow for video recording. Angel Hair pasta (DeCecco; Angel Hair No. 9) pasta was sterilized with ethidium oxide treatment. After sterilization, pasta was cut into 2.8cm lengths with markings every 0.7cm using Crayola Washable Marker (Broad Line Non-Toxic Markers, Classic Colors, 10 count). Mice showed no preference to marked or unmarked pasta and readily ate all pasta provided.

The following food restriction schedule was used during baseline training: night 1, mice were totally fasted; nights 2-5, mice received 5% chopped chow each night. The chow percentage was found by adding up the total weight of all mice in one cage, and then taking 5% of this value. Weight was carefully monitored over the study and was not allowed to drop within 85% of baseline weight. After injury during experimental time points, mice were fasted only overnight, ~18-22 hours. We found that after <18 hours fasting time, mice did not have an increased level of motivation to eat. Water was always provided *ad lib*.

The following baseline training schedule was used to determine paw preference: days 1-3, mice were introduced to single plane mirrors (10 cm diameter circle mirrors; Hobby Lobby) and pasta pieces in the home cage to minimize neophobic response, mirrors remained in the home cage for the duration of the experiment to continually acclimate mice to the reflective surface, as we found the mirrored bottom of the enclosure severely disrupted behavior without continued habituation; days 4-8, mice were habituated to the pasta handling enclosure for 20 minutes or the total length of eating time, whichever came first, and were given 3 test length (2.8cm) pasta pieces and as many short (0.7cm; maximum of 10 pieces) pasta pieces as possible during the remaining training time; days 9-13, mice were given 3 test length pasta pieces and timed for the total amount of eating time for all 3 pieces, during this time the “guide” and “grasp” paws were determined and recorded for each mouse.

The “guide” paw was the paw usually closest to the mouth when eating long pasta pieces and was used as the preferred paw for behavioral tests and contusion injury; the “grasp” paw was the paw further from the mouth when eating long pasta pieces (Tennant et al., 2010).

In this study, we attempted to determine the level of forelimb function for the preferred paw at different cervical SCI severities. We performed the pasta handling test each week and recorded mice eating 3 pieces of pasta in the enclosure (Sony Handycam HDR-CX440, Digital HD Video Camera Recorder). The time to eat each piece and total time in enclosure was recorded. The pasta handling test was not effective to determine forelimb function as after injury, instead of using the forelimb to reach and grasp the pasta as was predicted, mice instead used their mouth (“mouth pulling”) to pick up the pasta. Alternatively, the mouse would use the other paw, initially the “support” paw instead to handle pasta resulting in a “failure to contact” the pasta.

2.2.1.2. Single Pellet Reaching

The single pellet reaching test is a well-established method to assess forepaw and forelimb function in mice and rats (Farr and Whishaw, 2002; Xu et al., 2009; Wang et al., 2017). In this study, single pellet reaching was used to evaluate the function in the preferred paw after injury over a period of nine weeks. Mice were trained in the single pellet reaching task with a plexiglass skilled forelimb chamber (catalog #5401, Maze Engineers). Chocolate pellets (Product# F05301Dustless Precision Pellets, 20mg, Rodent Purified Diet; Bio-Serv) were used for the task and placed in a custom made pellet holder created by cutting off the end of a transfer pipette near the bulb (diameter = 1.3cm; height = 1.2cm) and mounting it on a flat plastic piece at a 25° angle. The holder was then attached to the pellet shelf using a binder clip.

The following food restriction schedule was used during baseline training: night 1, complete overnight fast (test within 20-22 hours); nights 2 and 4, mice received 2.5% chopped chow; nights 3 and 5, mice received 5% chopped chow. Food was returned promptly after testing and animals were

allowed full access for nights 6 and 7. The chow percentage was calculated as described in Section 2.2.1.1. Water was always provided *ad lib*.

The following baseline training schedule was used to determine paw preference and train animals in the skilled reaching task: days 1-3, pellets were dropped into the home cage to introduce the new food and minimize neophobic response; days 4 and 5, habituate mice in training enclosure with lots of pellets near reaching front for 15 minutes each day; days 6-20 fill pellet holder with 5-7 pellets and place centered to reaching hole, continuously refill holder so always containing 5-7 pellets and complete for 40 pellets or 15 minutes, whichever comes first, determine paw preference in reaching task and introduce the video recorder. We found it very important to allow the mice time to habituate to the video recorder as its initial presence reduced the number of pellets reached by 50% in some non-habituated animals. To speed this process up, a large black circle was cut from cardstock and taped to the home cage. The camera was placed on a tripod 7.2cm from the pellet reaching hole at a 30° angle.

In this study, we attempted to determine which of the kinematic steps of reaching and grasping were lost or preserved in different injury severities. We performed the single-pellet reaching test each week and recorded mice for 15 minutes or the total time for eating 40 pellets, whichever came first. The time to eat and number of pellets reached was recorded. The pellet reaching task was not effective because the mice used the uninjured paw for reaching instead, so in the future the holder should be offset to the reaching hole.

2.2.2. Locomotor Assessments

Mice were habituated and tested for 3 days in the rotarod (RR), complex horizontal ladder (cHL), and grooming tests 3 days prior to SCI. The RR, cHL, and grooming tests were completed after food was returned from forelimb testing and were performed every week beginning at 1wPI and

continuing until 9wPI. Animals were coded, and behavioral assessments and analyses were performed by two investigators blinded to the treatment groups.

2.2.2.1. Rotarod

The rotarod test is sensitive to deficits in coordination and locomotion (Stanley et al., 2005). The rotarod device (Ugo Basile) was set in 5 lanes with 5.5cm gaps for each lane and the time (seconds) on the rod was counted for each animal. Five trials were performed and the 3 highest scores were averaged for each animal. During baseline training, each mouse should perform above 120s per trial (Stanley et al., 2005). False starts, or scores <5 seconds, should not be counted except in the first week PI as some animals will be too injured to perform. The rotarod test was performed weekly and the average rotarod score for each mouse was calculated. As mice will fall off, especially in the weeks after injury, it is important to distinguish by careful observation if the mouse is jumping off or falling off of the rotarod.

2.2.2.2. Complex Horizontal Ladder (cHL)

The complex horizontal ladder (cHL) test is sensitive to locomotor deficits after cervical SCI as it requires adequate sensorimotor function to feel the ladder rungs and contact the rungs during stepping (Soblosky et al., 2001; Gensel et al., 2006; Metz and Whishaw, 2009). The device consists of a walkway enclosed by Plexiglas walls (8 cm tall, 80 cm long and 3.5 cm apart) raised 15 cm above ground (height of 2 empty, inverted rat cages). Wooden applicator sticks (1mm diameter) were inserted into holes drilled along the lower edge (every 0.5 cm) at random intervals to prevent memorization of the locomotor task, requiring an increased level of active engagement in the cHL task rather than spacing every 0.5cm as is traditional (Metz and Whishaw, 2009). Rungs did not shift or rotate while in place but were still easily removed after testing. Mice were habituated to the cHL apparatus in 3 training sessions where each session consisted of 5-10 complete transits. The ends of the runway were blocked off with red enrichment cylinders to prevent animals from escaping at the

end and to encourage the animal towards the “target” end point, which was the home cage placed at the end of the walkway. The animals were free to explore and move about the apparatus, and sugared cereal was available in a goal box at the left or right side (respective to MMS paw preference). The mice were trained to travel from the start point towards the goal box without turning around and, if required, gently guided by the experimenter. A testing session consisted of 1 successful walk without turning or backwalking and was recorded on a video camera angled perpendicular to the rungs. The percentage of missed steps ($\# \text{ misstep} / \# \text{ total steps} \times 100$) were calculated using slow motion video playback for each walk and the average of both walks was the percentage of missteps for each week.

2.2.2.3. Grooming

The grooming test is sensitive to sensorimotor deficits induced by cervical SCI and was performed as previously described (Bertelli and Mira, 1993; Soblosky et al., 2001). Briefly, cool tap water was applied to the animal’s head and back with soft gauze, and the animal was placed in a clean, clear glass cylinder (12.5cm diameter; 30 cm height; or a 4L beaker). Two mirrors were placed behind and beside the cylinder forming the back and left walls, respectively. The camera was placed 21cm diagonally from the corner made by the mirror intersection at the level with the cylinder bottom (0 degrees). Grooming activity was recorded with a video camera (Sony Handycam HDR-CX440, Digital HD Video Camera Recorder) for 2 minutes total. Scoring was done according to the highest point reached by the forelimb: 0, the animal was unable to contact any part of the face or head; 1, the animal’s forepaw touched the underside of the chin and/or the mouth area, but not the nose; 2, the animal’s forepaw contacted the area between the nose and the eyes, but not the eyes; 3, the animal’s forepaw contacted the eyes and the area up to, but not including, the front of the ears; 4, the animal’s forepaw contacted the front, but not the back, of the ears; 5, the animal’s forepaw contacted the area of the head behind the ears (full range of motion). Slow motion video playback was used to score each forelimb independently.

2.3. Anterograde Tracing for descending Long Spinal Tracts

Fifteen mice (3 groups; 5 mice/group) were used for anterograde tracing. After the final behavioral tests at 9 weeks following SCI, mice were again anesthetized with a mixed solution of ketamine and xylazine. A midline sagittal incision was performed to excise the skin and subdermal tissue away from the skull. A mouse micro drill was used to open the skull, and then mice were moved to a stereotaxic injection instrument with a micro glass needle to deliver either virus or BDA into the motor cortex, red nucleus, or reticular formation as described in Table 1. Mice were sacrificed after 3 weeks and the brain and spinal cord was removed and collected for histology.

Injections				
<i>Anterograde Tracer</i>	<i>Concentration</i>	<i>Injection Volume</i>	<i>Target Brain Region</i>	<i>Coordinating Spinal Tract</i>
AAV5-CAG-RFP	2.30E + 13 (gc/ml)	8 injection points; 0.25 uL/point	Contralateral Motor Cortex	Corticospinal Tract (CST)
AAV5-CAG-GFP	2.10E + 13 (gc/ml)	2 injection points; 0.5 uL/point	Ipsilateral Pontine Reticular Nucleus	Reticulospinal Tract (RtST)
Biotinylated Dextrin Amine	10% BDA	1 injection point; 1 uL/point	Contralateral Red Nucleus	Rubrospinal Tract (RST)

Table 1 | Anterograde tracers used in cortical injections. Concentrations, target brain region, and target coordinating spinal tract indicated in right columns.

2.4. Retrograde tracing by Cholera Toxin B

Fifteen mice (3 groups; 5 mice/group) were used for CBT tracing. At 9 weeks PI, mice were anesthetized with a mixed solution of ketamine and xylazine, and a midline dorsal laminectomy was performed at C7 to expose the spinal cord. Mice were moved to a stereotaxic injection instrument with a micro glass needle and Cholera Toxin B (CTB; Sigma, Catalog #C9903-2MG) was injected on the hemisection ipsilateral to the injury at C7 up and down (0.5uL/injection; 1% diluted in 1XPBS). Afterward, the incision was sutured in layers, bacitracin ointment (Qualitest Pharmaceuticals, Huntsville, Alabama, US) was applied to the wound area, 0.1 mL of gentamicin [stock solution 20 mg/ml, subcutaneous (sc); ButlerSchein, Dublin, Ohio, US] was injected, and the animals recovered on soft bedding on a water-circulating heating pad. Mice received a mixed solution of antibiotic, gentamicin, and analgesic agent, buprenorphine (0.05 mg/kg, sc; Reckitt Benckise, Hull, England), once a day for 3 days. Mice were monitored carefully post-operatively and were given 1-2mL Ringers saline solution (0.03% bacteriostatic saline, sc) if they appeared weak. Mice were sacrificed after 2 weeks and the brain and spinal cord were removed and collected for histology.

2.5. Immunohistochemistry

Two or three weeks after retrograde or anterograde tracing injections, respectively, mice were anesthetized with a mixed solution of ketamine (80 mg/kg, ip) and xylazine (10 mg/kg, ip), and perfused transcardially with 0.01 M phosphate buffered saline (PBS, pH 7.4), followed by 4% paraformaldehyde (PFA) in PBS. The injured spinal cord segments and brains were removed, post-fixed in 4% PFA overnight, cryoprotected in 20% sucrose overnight, and 30% sucrose overnight at 4° C and embedded in OCT compound (Fisher Scientific). The spinal cords were cryosectioned in 20 um slices either transversely or longitudinally and mounted serially (10 slides/series) on Super Frost Plus

Gold Slides. The cortex and midbrains were cryosectioned in 20 μ m slices coronally proceeding rostrally to caudally and mounted serially while skipping every 40 μ m (3 slides/series; ~3 series/block).

For immunofluorescent staining, slides were briefly warmed on a hot plate and then blocked with 10% donkey serum in 1XPBS containing 0.2% Triton X-100 (PBST) for 1 hour at RT. The sections were then incubated in PBST containing 5% donkey serum and either triple-stained with 1) polyclonal goat anti-mCherry (mChy; a marker for red fluorescent protein; 1:400; Sicgen), polyclonal chicken anti-Green Fluorescent Protein (GFP; a marker for green fluorescent protein; 1:400; Chemicon), and CY5-streptavidin (CY5-strep; a marker for biotinylated dextran amine also called BDA; 1:200; Jackson ImmunoResearch Lab); 2) polyclonal rabbit anti-mChy (1:200; Abcam), polyclonal chicken anti-GFP (1:400; Chemicon), and polyclonal goat anti-Cholera Toxin B Subunit (CTB; marker for spinal retrograde tracing; 1:10,000; List Biological Labs #703); 3) rat monoclonal anti-glial fibrillary acidic protein (GFAP; a marker for reactive astrocytes; 1:200; Invitrogen), polyclonal chicken anti-microtubule associated protein 2 (MAP2; a marker for neuronal parikarya and dendrites, 1:500; Millipore), and rabbit polyclonal anti-fibronectin (FN; a marker for fibronectin in the injury core; 1:200; Sigma); or double-stained with polyclonal goat anti-CTB (1:10,000; List Biological Labs) and polyclonal rabbit anti-neuronal nuclei (NeuN; a marker for the nucleus of mature neurons; 1:1,000; Millipore); or single-stained with 1) polyclonal rabbit anti-FN or 2) polyclonal chicken anti-MAP2 overnight at 4° C (Table 2).

After three washes of 5 min in PBS, sections were incubated in PBST containing 5% donkey serum, donkey anti-goat IgG Rhodamine Red-X (1:200; Jackson-lummonRes Lab; Baltimore, MD, United States), donkey anti-chicken IgY (IgG) FITC-conjugated F(ab')₂ fragments (1:200), donkey anti-rabbit TRITC-conjugated IgG (1:200), donkey anti-rat TRITC-conjugated IgG (1:200), donkey anti-goat Cy5-conjugated IgG (1:200), donkey anti-rabbit Cy5-conjugated IgG (1:200), or donkey anti-chicken Cy5-conjugated IgY (IgG) F(ab')₂ fragments (1:200) for 1 h at RT. Hoechst 33258 (1:1000; 20mM,

Anaspec; Cat. #AS83219) was used to stain nuclei during secondary antibody incubation. The sections were rinsed in PBS and coverslipped with ProLong® Gold antifade reagent. A Zeiss AxioObserver Z1 inverted fluorescence microscope was used to capture representative images at 10x and 20x resolution. Photomicrographs were assembled using ImageJ (v.1.52p, NIH) and Inkscape (v.1.0).

Primary Antibodies			
<i>Material</i>	<i>Dilution</i>	<i>Source</i>	<i>Catalog Number</i>
Chicken polyclonal anti-glial fibrillary acidic protein (GFAP)	1:200	Millipore	AB5541
Chicken polyclonal anti-green fluorescent protein (GFP)	1:400	Chemicon	AB16901
Chicken polyclonal anti-microtubule associated protein 2(MAP2)	1:500	Millipore	AB5543
Goat polyclonal anti-Cholera Toxin B Subunit (CTB)	1:10,000	List Biological Labs	#703
Goat polyclonal anti-mCherry (mChy)	1:400	Sicgen	AB0081-200
Mouse monoclonal anti-GFAP	1:400	Sigma	G3893
Rabbit polyclonal anti-fibronectin (FN)	1:200	Sigma	F3648
Rabbit polyclonal anti-GFAP	1:400	DAKO	Z0334
Rabbit polyclonal anti-mChy	1:200	Abcam	16743
Rabbit polyclonal anti-neuronal nuclei (NeuN)	1:1,000	Millipore	ABN78
Rat monoclonal anti-mouse CD68	1:200	Bio-Rad	MCA1957GA
Rat monoclonal anti-GFAP	1:200	Invitrogen	13-0300
CY5-Streptavidin	1:200	Jackson ImmunoResearch	016-170-084

Table 2 | Primary antibodies used in immunofluorescent histology staining and imaging. Dilutions, vending company, and catalog number indicated in right columns.

2.4. Histological Analysis

To assess the anatomical effects of graded spinal cord injury, IHC images were quantified for injury size, gray matter lost, and CTB neurons.

2.4.1. Quantification of Injury Size – Fibronectin

Injury size was quantified in ImageJ (NIH) using the average of 3 longitudinal samples that had the largest areas of fibronectin (FN) immunoreactivity (IR). Transverse longitudinal images were captured every 200um for all slices with FN-IR staining 20x resolution on a Zeiss AxioObserver Z1 inverted microscope with the tiling and stitching function. For the longitudinal quantification, the sample with the greatest area of FN-IR and one adjacent section rostrally and caudally was measured for each animal using an area average approach (Soderblom et al., 2013; Jeong et al., 2017). The largest area was found by outlining the bright FN+ staining in ImageJ with a freehand drawing tool and then automatically measured and the value recorded. The FN-IR average of each group was found to give the size of injury.

Five mice were in each injury group (3 groups total). Of the fifteen spinal cords analyzed, one mouse from the 50kD injury group was excluded due to tissue damage during histological processing.

2.4.2. Quantification of Gray matter Loss – MAP2

The amount of gray matter lost by microtubule associated protein 2 (MAP2) in longitudinal samples was calculated by a subvolume approach (Oorschot, 1994; Cao et al., 2005) in ImageJ. Transverse longitudinal images were captured every 200um for the entire thickness of the spinal cord using 10x resolution on a Zeiss AxioObserver Z1 inverted microscope with the tiling and stitching function. The region of interest (ROI) for each slice was found by using a rectangular selection which limited the image to a 4mm length (2mm rostral and caudal to the epicenter; rectangle midline at epicenter) containing both the ipsilateral and contralateral widths. The epicenter was defined by the region of MAP2-IR negative area midway through the spinal cord containing DAPI clustering at the

epicenter of the injury area. Once the ROI was defined, the image was converted to 8-bit format, thresholded to only include the MAP2-IR areas, and the thresholded area was measured automatically by ImageJ and the value was recorded for each slice containing MAP2 in a sample (approximately 5-8 slices per sample). Each slice was multiplied by the distance to the adjacently analyzed slice (200um) to generate a subvolume for each slice of the spinal cord (5-8 slices per spinal cord). The subvolumes were summed together to create a total gray matter volume for each animal. The MAP2-IR volume of the control animals was averaged together, and the volume of gray matter lost was found by subtracting the MAP2-IR volume of each injury animal from the MAP2-IR average volume of the control animals (Gray matter Lost = Control MAP2-IR Average – Injury Animal MAP2-IR).

Five mice were in each injury group (3 groups total) and three spinal cords from control mice without injury were used. Of the eighteen spinal cords analyzed, 3 were removed due to tissue damage during histological processing; one animal from the 70kD group and two animals from the 50kD group.

2.4.3. Quantification of descending Propriospinal Spinal Tracts by CTB retrograded tracing.

The number of descending propriospinal neurons rostral to the injury were quantified in samples 2mm rostral (R2mm) to the lesion (approximately C3, or 2000um rostral to the epicenter) in ImageJ. Cross-sectional images were captured using 20x resolution on a Zeiss AxioObserver Z1 inverted microscope with the tiling and stitching function. The image used for counting was created by exporting each channel for NeuN and CTB separately (Rhodamine and CY5, respectively). The brightness and contrast for NeuN was adjusted to exclude the high background levels due to poor cryopreservation. The CTB channel image was converted to 8-bit and the NeuN image was overlayed at 15% opacity. CTB-IR neurons were counted manually in ImageJ using the Cell Counter Plug-in for the ipsilateral and contralateral sides separately for each animal and the values recorded.

2.5. Statistical Analysis

Statistical analyses were performed with SPSS v.25 (behavioral RM ANOVA, post-hocs; IHC analysis) or GraphPad Prism v.8 (regressions and correlations). Graphs represent the mean \pm standard error of the mean. Behavioral and histological quantification graphs were made in Microsoft Excel and heat maps and correlational plots were generated in GraphPad Prism.

2.5.1. Behavioral Statistics

All forelimb and locomotor behavioral testing was performed before injury as a baseline and again 1wPI to ensure adequate injury deficit in locomotion. All analyses were performed by experimenters blinded to the treatment groups.

The mean cHL misstep percentages, RR and grooming scores were tallied by experimental group and plotted as a function of time PI. Performance change over time for cHL misstep percentage and RR score was analyzed using repeated-measures ANOVA with the between groups factor. The differences among the groups and each group over the 9wPI testing weeks were performed using Tukey's Honestly Significant Difference (HSD) *post hoc* test and one-way ANOVA.

The mean grooming scores were tallied by experimental group and plotted as a function of time PI. Grooming score change over time was analyzed using the Kruskal-Wallis *H*-test.

2.5.2. IHC Statistics

The mean area of FN and mean volume of MAP2 were tallied by experimental group by experimenters blinded to the group. The differences of MAP2 and FN between injury groups were statistically analyzed in SPSS v.25 using a one-way ANOVA with Tukey's HSD *post hoc*.

2.5.3. Correlation plots

The relationship of behavioral test to histology outcome was analyzed in GraphPad Prism for rotarod vs. fibronectin, rotarod vs. MAP2, cHL vs. FN, cHL vs. MAP2, grooming vs. FN, and grooming vs. MAP2. A simple linear regression was performed to assess the rate of change in behavioral

performance for each animal from 1-9 weeks PI, which was given by the best-fit slope value. D'Agostini-Pearson and Shapiro-Wilk tests were performed to assess if distribution was normal or lognormal in fit. All data were normally distributed so the Pearson correlation test was used to assess the correlations of injury severity, slope of behavioral tests, and IHC data. An additional set of tests to assess normality and correlation following the same parameters for normality and correlational testing were performed separately to test the behavioral scores at 9wPI with the histology values and injury severities. Correlations were considered weak if $r_p = <0.6$, moderate if $r_p = 0.6-0.8$, and strong if $r_p = >0.8$.

Chapter 3 – RESULTS

Increasing the severity of SCI contusion results in more missteps in complex horizontal ladder

To test the effects of graded unilateral cervical contusion on locomotor deficits, animals were assessed weekly using the complex horizontal ladder (cHL) (Soblosky et al., 2001; Gensel et al., 2006; Metz and Whishaw, 2009). The cHL test measures the number of missteps an animal makes over a horizontal ladder missing rungs at irregular intervals, creating an uneven rung pattern encouraging the animal to actively participate in the assessment to prevent missteps rather than walking using typical gait (Metz and Whishaw, 2009). Normally, uninjured mice are able to perform with 25% missteps or less, so we used 25% as our baseline threshold and confirmed each mouse was capable of <25% missteps prior to injury. Following SCI, sensorimotor function is significantly impaired and the ability to step correctly is reduced, resulting in an increase in missteps in the cHL.

Differences in the percentage of missteps between the 50, 70, and 90kD groups over the nine weeks of behavioral testing were assessed using a Repeated Measures ANOVA and Tukey's Honestly Significant Difference (HSD) *post hoc* testing with the between subjects factor as experimental group and the within subjects factor as repeated measures on time. The effects of time and group on the percentage of missteps were significant ($p = <0.000$ and $p = <0.000$, respectively); a Greenhouse-Geisser adjustment for sphericity was used to account for variance. The interaction of time and group was also significant ($p = 0.037$). This indicates that contusion severity had different effects on the percentage of missteps depending on the week post-injury (PI), so follow-up one-way ANOVA's with multiple comparisons by Tukey's HSD *post hoc* testing was performed (Figure 4). The percentage of missteps was significantly increased in the 70kD group compared to the 50 kD group at 1-3 weeks PI. The 90kD group had significantly more missteps than the 50kD and 70kD group at all 1-9 weeks PI. All groups had an increased number of missteps after SCI. The percentage of missteps in cHL were directly related to injury severity. Specifically, as the force of contusion severity increased (kD), the

number of missteps also increased. The percentage of missteps in the preferred forelimb improved significantly over time in the 90kD group from 1 to 7 weeks PI ($F = 33.199$, $p = <0.000$) and in the 50kD group from 1 to 6 weeks PI ($F = 176.495$, $p = <0.000$). The 70kD group had not yet reached a plateau in cHL performance and was still improving at 8 weeks PI ($F = 163.07$, $p < 0.000$).

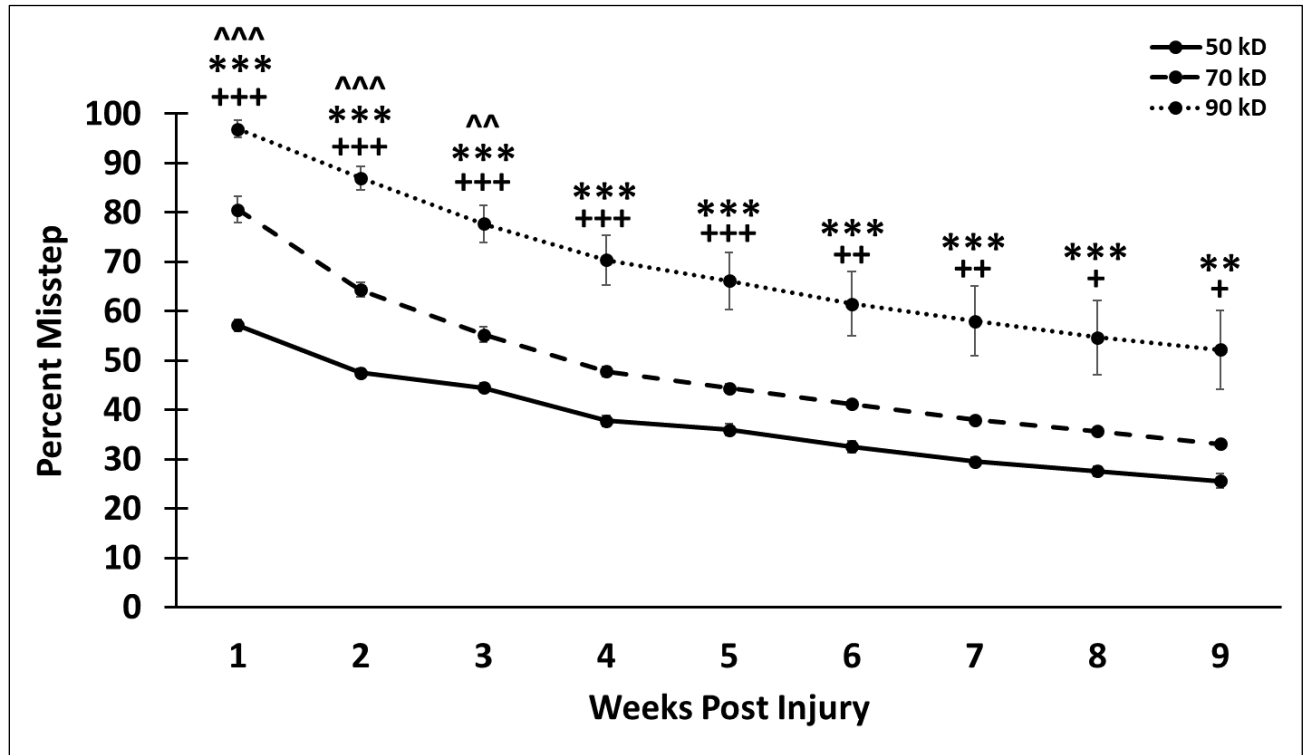


Figure 4 | Percentage of missteps for complex horizontal ladder (cHL) for 9 weeks post-injury (PI) for mice in 90kD, 70kD, and 50kD groups after unilateral contusion spinal cord injury (SCI). Mice in all injury grades had impaired stepping ability on the paw ipsilateral to the lesion. There were significant differences in the percentage of missteps in the one-way ANOVA at all weeks PI. Results represent mean \pm standard error of the mean; $n = 10$ mice per group. $^{\wedge\wedge}P < 0.01$, $^{\wedge\wedge\wedge}P < 0.001$ represent 70kD $>$ 50kD; $^{**}P < 0.01$, $^{***}P < 0.001$ represent 90kD $>$ 50kD; $^{+}P < 0.05$, $^{++}P < 0.01$, $^{+++}P < 0.001$ represent 90kD $>$ 70kD.

Contusion severity reduces time in rotarod score

To test how the ability to perform the rotarod test was affected by graded SCI, animals were assessed weekly in the rotarod test. The rotarod test assesses for forelimb and sensorimotor function and is sensitive to locomotor deficits (Stanley et al., 2005). The rotarod test measures the time spent on the rotarod, a spinning rod in midair with gradually increasing speed, from placement to drop time. Normally, uninjured mice can walk >120 seconds (Stanley et al., 2005), so we used 120 seconds as our baseline threshold to make sure all mice were capable of walking at least this time length. Following SCI, sensorimotor function is impaired so mice will fall off the rotarod easier, reducing the amount of time spent on the rotarod and lowering the score.

Differences in rotarod score between the 50, 70, and 90kD groups over the nine weeks PI were assessed using a RM ANOVA and Tukey's HSD *post hoc* testing with the between subjects factor as experimental group and the within subjects factor as repeated measures on time. The effects of time and group on rotarod score were significant ($p = <0.000$ and $p = 0.0003$, respectively); a Greenhouse-Geisser adjustment for sphericity was used to account for variance. The interaction of time and experimental group on rotarod score was also significant ($p = 0.026$). This indicates that contusion severity effected the rotarod score depending on the week PI, so follow-up one-way ANOVA's with multiple comparisons by Tukey's HSD *post hoc* testing was performed (Figure 5). The 70kD group had lower rotarod scores than the 50kD group at 8 and 9 weeks PI. The 90kD group had significantly lower rotarod scores than the 50kD group at all 1-9 weeks PI. The 90kD group also had significantly lower rotarod scores compared to the 70kD group at weeks 3, 4, and 8 weeks PI.

All groups had a reduced rotarod score after SCI. The rotarod scores by seconds were inversely related to injury severity. Specifically, as the contusion force increased (kD), the seconds on the rotarod decreased. The rotarod scores improved significantly in the 90kD group from 1 to 3 weeks PI ($F = 27.816$, $p = <0.000$), in the 70kD group from 1 to 5 weeks PI ($F = 43.095$, $p = <0.000$), and in the

50kD group from 1 to 5 weeks PI ($F = 40.28$, $p = <0.000$). There was no marked improvement in rotarod score after 6 weeks PI in any injury group.

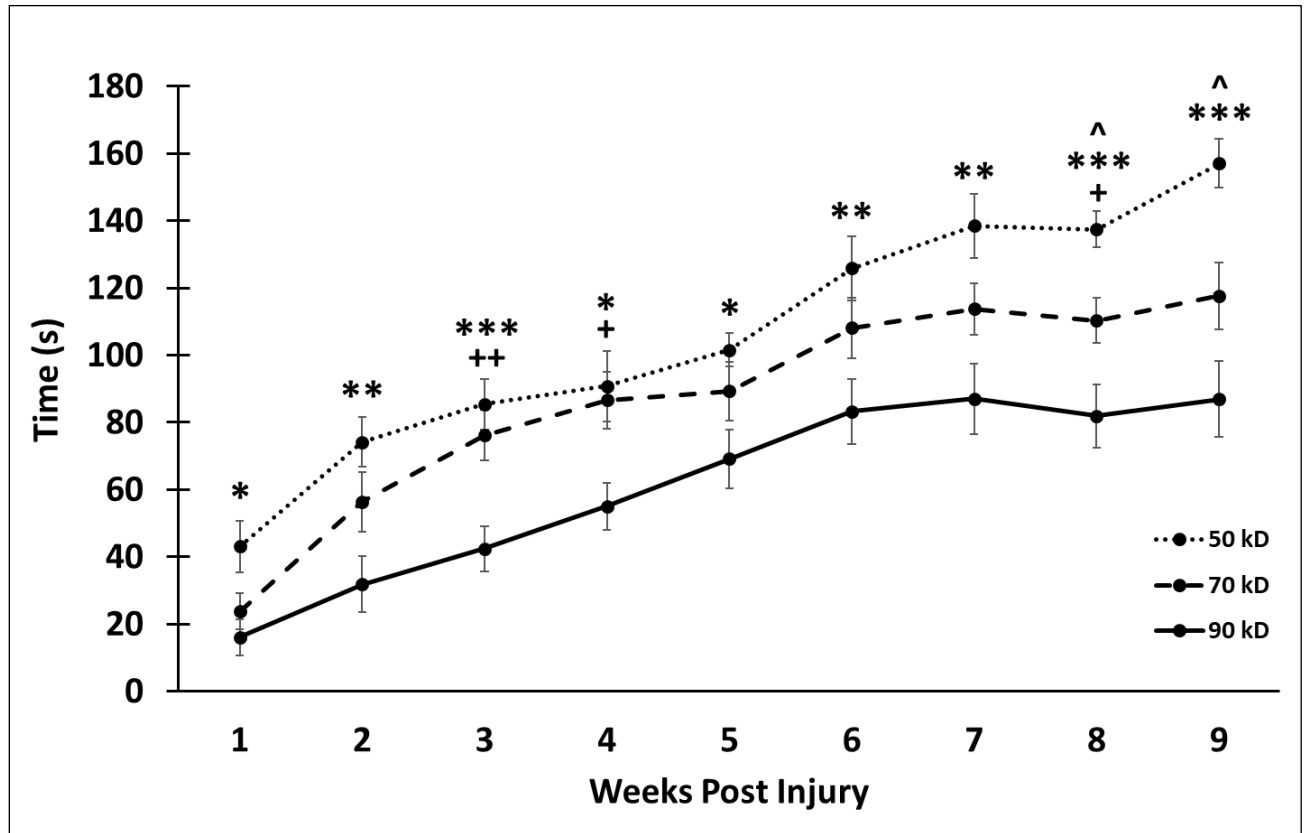


Figure 5 | Time score for rotarod for 9 weeks post-injury (PI) for mice in 50kD, 70kD, and 90kD groups after unilateral contusion spinal cord injury (SCI). All groups had impaired performance in the rotarod due to injury and fell off the rod easier than uninjured animals, which typically score at least 120 seconds or more (Stanley et al., 2005). There were significant differences in rotarod score in the one-way ANOVA at all weeks PI. Results represent mean \pm standard error of the mean; $n = 10$ mice per group. $^{\wedge}P < 0.05$ represent 70kD < 50kD; $*P < 0.05$, $**P < 0.01$, $***P < 0.001$ represent 90kD < 50kD; $+P < 0.05$, $++P < 0.01$ represent 90kD < 70kD.

Grooming score reduced in all injury severity groups after unilateral contusion

To test if injury severity impaired grooming ability, animals were assessed weekly in the grooming test (Bertelli and Mira, 1993; Soblosky et al., 2001). The grooming test is typically used to assess sensorimotor deficits in mice and rats after peripheral, spinal, or cortical injury and can largely detect functional deficits. The grooming test measures the functional cleaning ability in a forepaw using a scoring system based on how high the mouse can reach up its face, and is scored 0-5. Normally, uninjured mice can score between 4 and 5, indicating the cleaning ability to the forehead and behind the ears. During our baseline analysis, we found that mice typically scored around a 4 as was consistent with other cervical SCI mice studies (Hilton et al., 2013), so we used 4 as our baseline threshold to make sure all mice could clean to the forehead. This indicates that mice might already be performing lower than the “standard” even at the baseline testing.

Differences in grooming score between the 50, 70, and 90kD groups over the nine weeks PI were assessed using a Kruskal-Wallis test with follow-up pairwise comparisons adjusted with a Bonferroni correction for multiple tests. Significant differences were found at 1 ($p = 0.018$), 2 ($p = 0.030$), 8 ($p = 0.029$), and 9 ($p = 0.015$) weeks PI. The 90kD group had significantly lower grooming scores than the 50kD group at 1 ($p = 0.043$) and 9 ($p = 0.036$) weeks PI. The 90kD group had significantly lower grooming scores than the 70kD group at 1 ($p = 0.043$), 8 ($p = 0.034$), and 9 ($p = 0.036$) weeks PI. Overall comparisons at 2 weeks PI indicated significance but there were no significant differences found at the pairwise comparisons level.

All groups had reduced performance in grooming after SCI in the ipsilateral side while the contralateral side was unaffected. The grooming scores were not obviously related to injury severity. Specifically, with increased contusion force (kD), the 90kD group performed overall worst but the 50 and 70kD groups performed largely similarly. The grooming scores improved moderately over the study for some animals, and the maximum grooming score achieved in any group was a 2 while the

lowest was a 0. Most animals scored a 1 at any time point PI, suggesting that the grooming test is not as sensitive as the rotarod and cHL to deficits after graded cervical SCI.

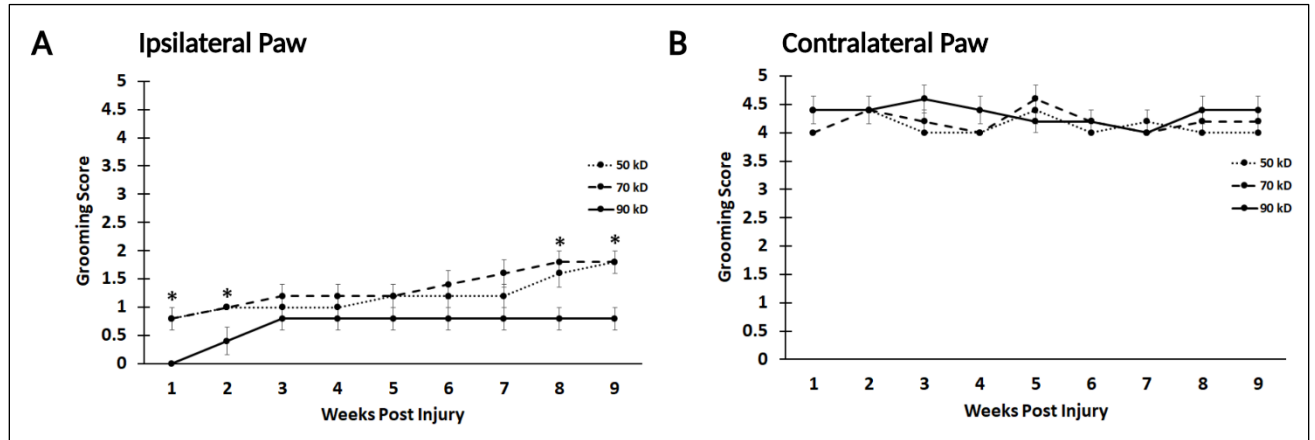


Figure 6 | Grooming scores for 9 weeks post-injury (PI) for mice in 50kD ($n = 5$), 70kD ($n = 5$), and 90kD ($n = 5$) groups after unilateral contusion spinal cord injury (SCI). Mice in all injury grades lost forelimb function in the paw ipsilateral **(A)** after injury, while the contralateral paw **(B)** was unaffected. Results represent mean \pm standard error of the mean (SEM); * $p < 0.05$.

The effect of graded SCI on forelimb function in pasta handling and single pellet reaching

To test if forelimb function in task specific assessments was affected after graded cervical hemiconfusion, animals were trained before injury in the pasta handling (Allred et al., 2008; Tennant et al., 2010; Whishaw et al., 2017) and single pellet reaching (Farr and Whishaw, 2002; Xu et al., 2009; Wang et al., 2017) tasks. The pasta handling test has been used to assess deficits in forelimb function in mice (Tennant et al., 2010) and rats (Allred et al., 2008; Tennant et al., 2010; Whishaw et al., 2017). The single pellet reaching task has been used to analyze the kinematic movements in reaching and grasping in fine kinesthetic detail (Farr and Whishaw, 2002) with great success. The single-pellet reaching task has well been established as a “gold standard” in forelimb function (Farr and Whishaw, 2002).

In pasta handling, normally mice handle long pieces of pasta by using a designated paw as a “guide” and place this paw on the end of the pasta proximal to the mouth and place the “grasp” paw farther away at the distal end of the pasta. For short pieces, mice usually keep their paws together at the same distance on the pasta (Tennant et al., 2010). Impaired reaching typically involves a switching of the guiding and grasping paws, holding the paws together on long pieces and apart on short pieces, or changes finger orientation when gripping the pasta. The pasta handling task was not efficient at detecting forepaw reaching and grasping specific deficits after SCI. Rather than using any “atypical” reaching behaviors such as altering the finger placement or gripping patterns on the pasta, the mice used their uninjured paw and mouth to pick up and eat the pasta, making quantification largely impossible. We used this task by allowing the mice to finish 3 pieces of pasta without a time limit, and in the future using a time limit of 15 or 20 minutes would be extremely prudent to reduce time cost in this experiment. This assessment may work better in SCI rats or in head-fixed mice after SCI.

In pellet reaching, normally mice perform 10 steps during a reaching and grasping attempt (Farr and Whishaw, 2002). Mice will typically have a preferred paw that they will almost always use

for reaching; this was the paw injured in our SCI model. Impaired reaching and grasping involves missing steps or misperforming steps of the reach and grasp. The pellet reaching task was not efficient at detecting forepaw deficits in reaching and grasping after SCI and instead of using the preferred paw, mice would use their opposite paw. In another group of animals, we tried to offset the pellet holder which would force the mouse to use their preferred paw, but mice were unable to reach the pellets due to SCI even in mild injury groups (50kD). We used this task by allowing mice to reach for 40 pellets or after being in the enclosure for 15 minutes, whichever came first. We strongly suggest an automated method to perform pellet reaching as actively placing pellets individually is limiting on the researcher and is a high time cost at the beginning of the experiment during training. Pasta handling and pellet reaching may be useful in models of graded cervical SCI in rats or in head fixed mice, but in our hands these tests were not effective to detect differences in forelimb performance between injury grades.

Overview of histological changes after graded unilateral cervical contusion

The cervical unilateral hemicontusion in mice resulted in the formation of an astroglial scar with a fibrotic core. The lesion extended from the epicenter rostrally and caudally as determined by triple staining using fibronectin, a marker for fibroblasts in the lesion core; microtubule associated protein 2 (MAP2), a neuron specific marker; and glial fibrillary acidic protein (GFAP), a marker for reactive astrocytes (Figure 7). GFAP defined the lesion border while fibronectin defined the lesion core by filling in the cavity. Gray matter loss was defined by MAP2 and was evident ipsilaterally and mildly present on the contralateral side.

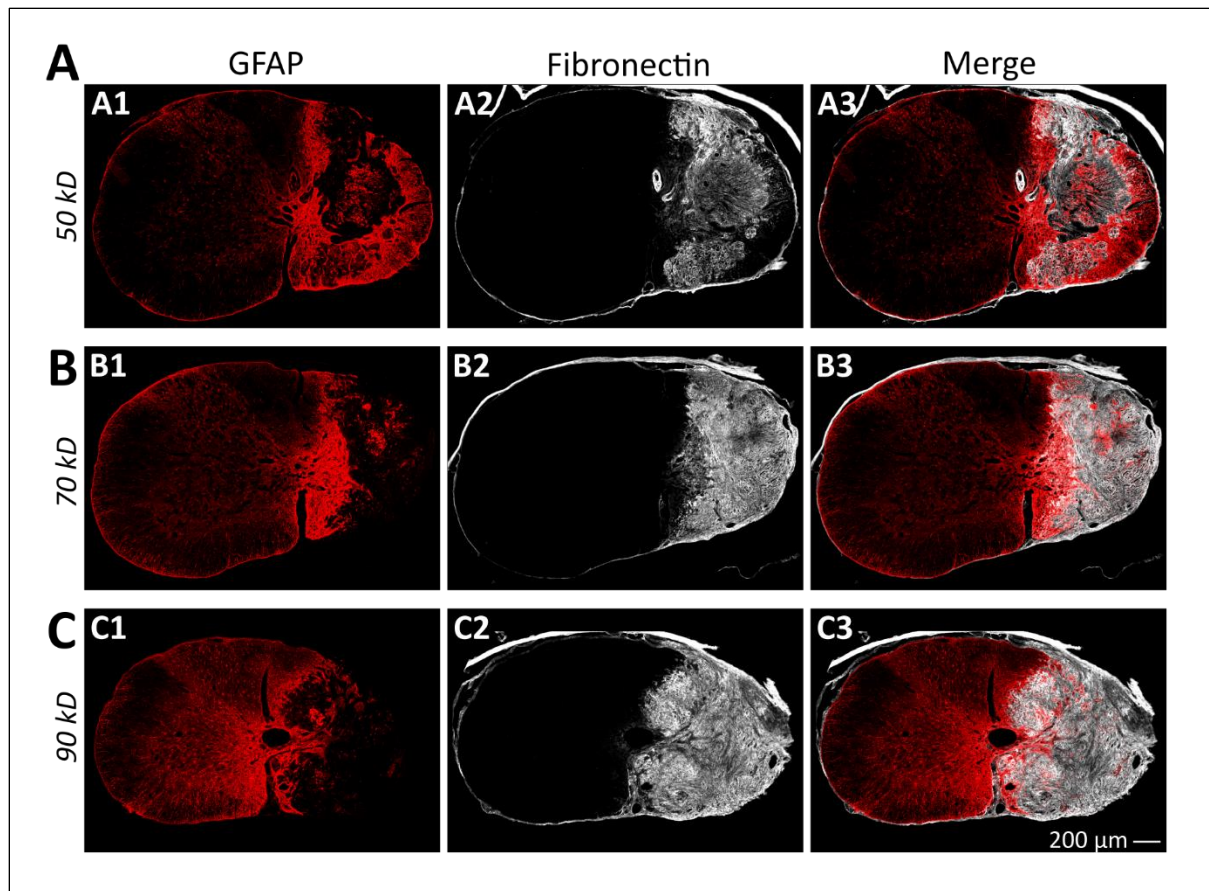


Figure 7 | Overview of histological effects of cervical hemicontusion spinal cord injury (SCI). Injury size was evaluated by immunohistochemistry staining against fibronectin (A2, B2, C2). The hemicontusion resulted in the formation of an astroglial scar with a large fibrotic core in all animals. Glial fibrillary acidic protein (GFAP) is a marker for reactive astrocytes that become hypertrophied after injury and can be seen throughout the white and gray matter (A1, B1, C1) and heavily concentrated around the fibrotic core forming an astroglial border around the fibrotic scar (A3, B3, C3). Representative images of the epicenter were taken for animals in the 50kD (A), 70kD (B), and 90kD (C) groups. Scale bar = 200μm.

Injury size by fibronectin is significantly greater in 70 and 90 kD contusion SCIs compared to 50 kD

To assess injury size, we used fibronectin, which is a well-established marker of the fibrotic core of the glial scar formed after contusive SCIs (Jeong et al., 2017; Cooper et al., 2018), allowing for a reliable measure of injury size (Figure 8). We found that the area of fibronectin extended farther rostrally and caudally in the 90kD animals than the 50 or 70kD animals when visualized in longitudinal sections. The 50 and 70kD mice formed a fibrotic scar that was more spherical rather than elliptically elongated as in the 90kD group.

Differences in fibronectin area between the 50, 70, and 90kD groups were assessed by a one-way ANOVA with the between groups factor. The area of fibronectin was significantly different between the injury groups ($p = 0.0001$), so follow-up multiple comparisons by Tukey HSD *post hoc* testing were performed. There was significantly more fibronectin in the 70kD group compared to the 50kD group ($p = 0.009$). The 90kD group had significantly more fibronectin than the 50kD group ($p = 0.00009$) and the 70kD group (0.021). Our data showed that injury size shown by fibronectin-IR area is closely related to injury severity ($r_p = 0.90$, $p = 0.00002$), suggesting fibronectin is a reliable marker of injury severity in mice.

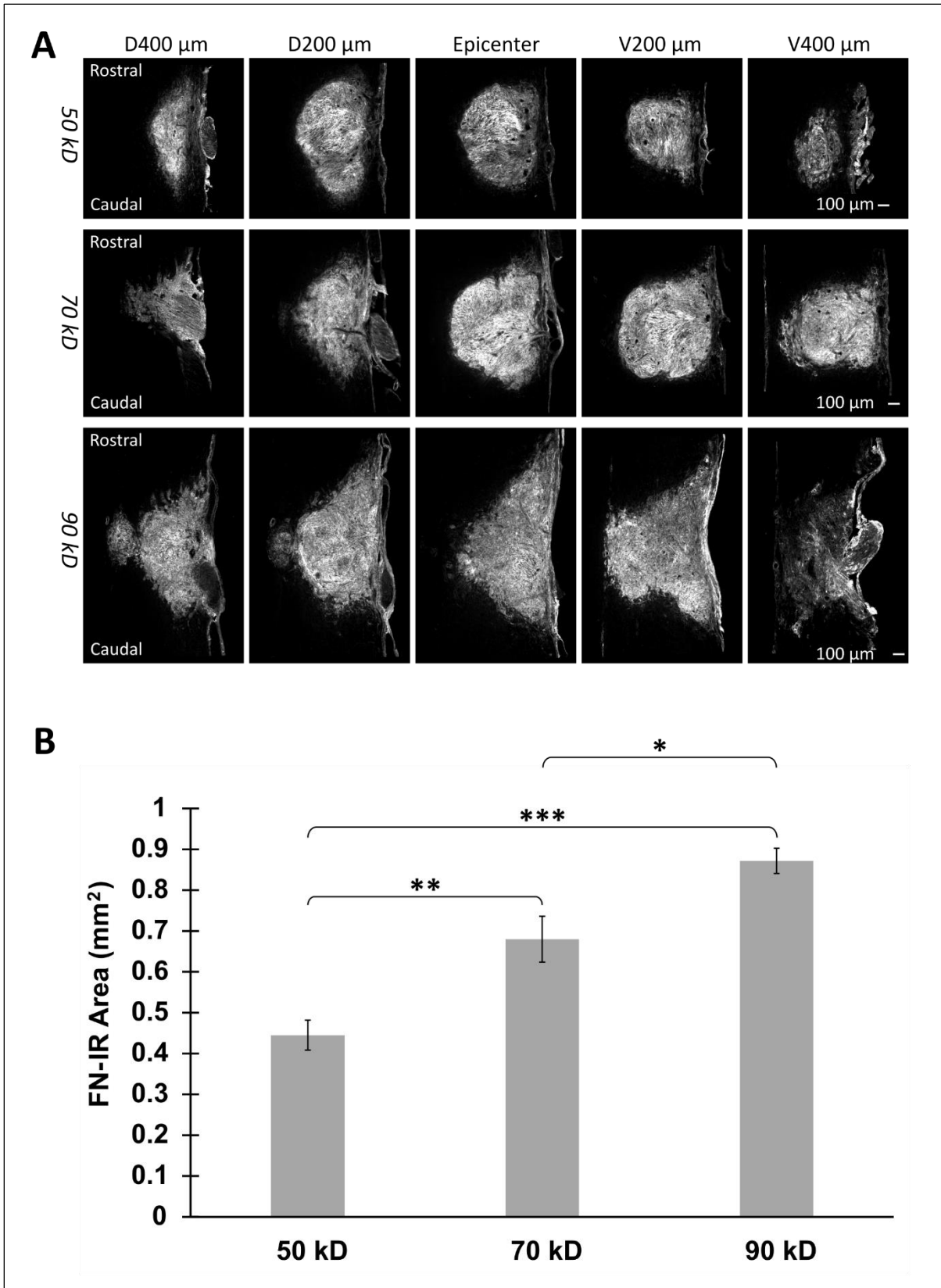


Figure 8 | Injury area by fibronectin-IR (mm^2) in longitudinal samples after graded unilateral cervical

contusion. Representative images (A) of the fibronectin (FN)-immunoreactivity (IR) cells in the injury center at 400 and 200um dorsal (D), 400 and 200um ventral (V), and the epicenter in animals with either 50, 70, or 90 kD unilateral contusion injuries. The quantification of the injury size (B) showed that animals with more severe contusions had significantly larger lesion ($p = 0.021$, 0.00009 , and 0.009 , respectively). Results in (B) represent mean \pm standard error of the mean; $n = 5$ per group. Scale bar = 100um. $*P < 0.05$, $**P < 0.01$, $***P < 0.001$.

Gray matter loss significantly increases after cervical contusion SCI

To assess gray matter loss, we quantified the lost volume of immunoreactive MAP2, a marker for neuronal perikarya and dendrites. Typically, MAP2 will stain the gray matter “butterfly” in spinal cord cross-sections or the left and right gray matter columns of longitudinal sections (Figure 9). SCI results in neuronal loss and a reduction in gray matter volume at the injury center.

The difference in gray matter loss in injury groups compared to the control group was assessed using a one-way ANOVA with the between groups factor. The area of MAP2 was significantly different between the injury group and control group ($p = <0.000$), so follow-up multiple comparisons by Tukey HSD *post hoc* testing was performed. There was a significant amount of gray matter loss in the 50kD group ($p = <0.000$), the 70kD group ($p = <0.000$), and the 90kD group ($p = <0.000$) compared to the control group, indicating a significant gray matter loss in all injury groups.

The difference in gray matter lost between injury groups was assessed using a one-way ANOVA with the between groups factor. The area of MAP2 was significantly different between the injury groups ($p = 0.0001$), so follow-up multiple comparisons by Tukey HSD *post hoc* testing were performed. There was significantly more gray matter loss in the 90kD group compared to the 50kD group ($p = 0.0004$) or the 70kD group ($p = 0.0004$). There was no significant difference in gray matter loss between the 50kD or 70kD group compared to the other injury animals. The lost volume of gray

matter depends on both the injury area in the epicenter and the distance the injury spreads rostrocaudally. The distance of the longer injury observed in 90 kD group longitudinal section may lead to the significantly larger lost volume of gray matter in this group. Gray matter loss correlates with injury severity ($r_p = 0.85$, $p = 0.0005$).

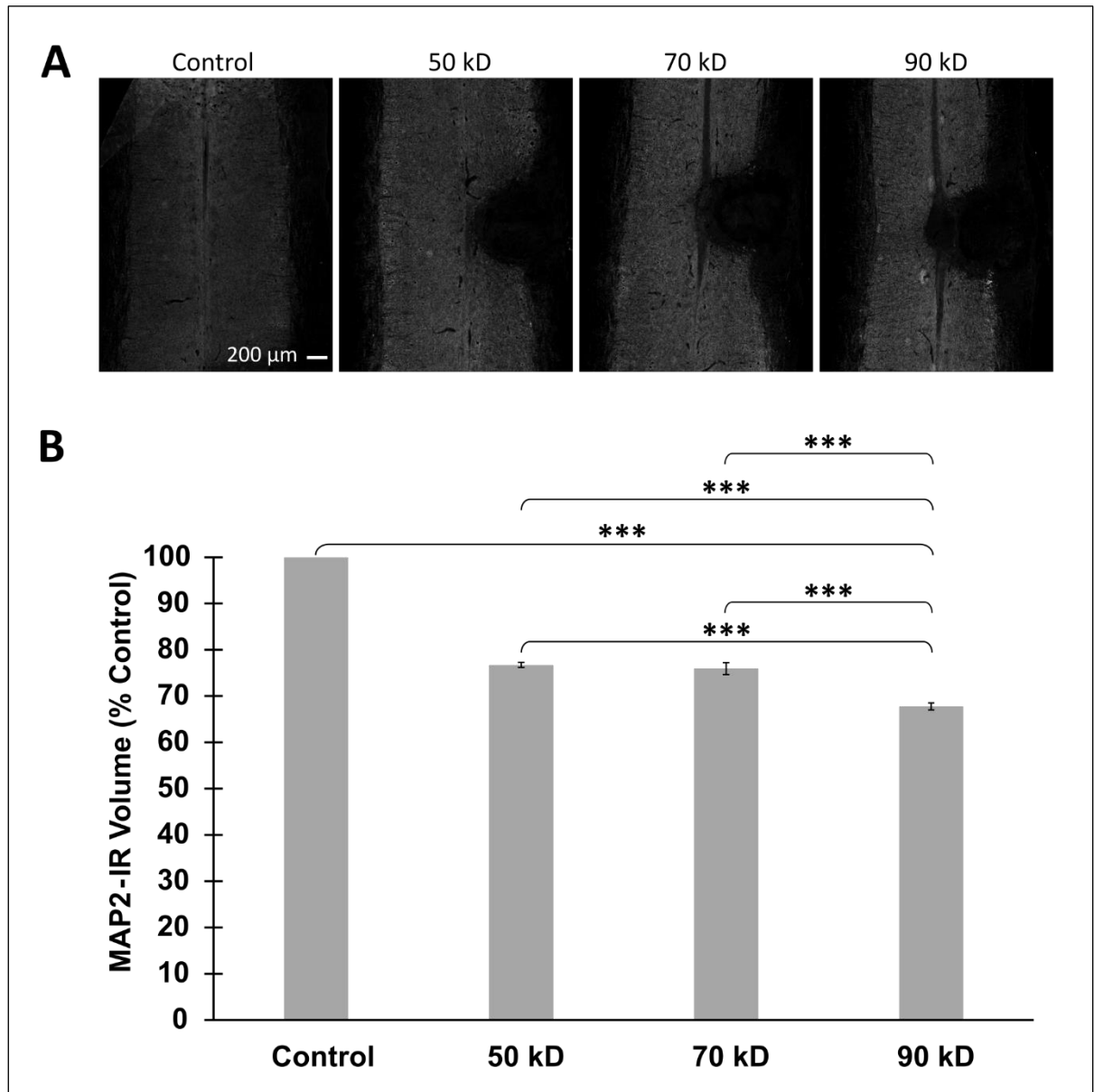


Figure 9 | Effect of cervical contusion on gray matter. Gray matter volume lost quantified (E, graph) by MAP2 (mm^3) in longitudinal samples (A) in 50kD ($n = 3$), 70kD ($n = 4$), and 90kD ($n = 5$) after graded

cervical contusion at C5. The subvolume of MAP2 (white) was quantified and summed for each sample to find the total volume, which was then subtracted from the gray matter volume of control animals (n = 3; D) Results represent mean +/- SEM. Scale bar =200 μ m. *** $p < 0.001$. Scale bar = 200um.

The propriospinal tracts after graded SCI by CTB retrograde tracing.

Descending propriospinal tracts (dPSTs) reside in the white matter of the spinal cord along with long descending tracts, while cell bodies reside in the gray matter. Propriospinal tracts connect neurons within spinal cord between segments for short distances (i.e. between C3 and C5) or long distances (i.e. between cervical and lumbar) (Laliberte et al., 2019). The long descending tracts include corticospinal (CST), reticulospinal (RtST), and rubrospinal tracts (RST) (Haines et al., 2018). In mice, the CST is located dorsomedially to the central canal; the Rostral RtST sits ventromedially and the caudal RtST sits ventrolaterally; the RST sits dorsolaterally and is anterolateral to the dorsal horn (Watson and Harrison, 2012). The long descending tracts in the white matter, are affected by contusion SCIs (Cao et al., 2005; Nishi et al., 2020), but the effect of SCI on dPSTs is not yet characterized. In this study, we completed the CTB tracing and will finish the quantification later to investigate whether different injury severities could cause differential loss in dPSTs between rostral cervical (C2-4) to caudal cervical (C6-7) after C5 graded SCI. We will further investigate how dPST loss could contribute to the different functional deficits after graded contusion SCI.

CTB was injected into C6-C7 to retrogradely label dPST neurons in the rostral cervical spinal cord in normal animals and injury animals after graded cervical unilateral contusion SCI (Figure 10, 11). Our results confirmed CTB as an effective retrograde tracer labeling dPST neurons in cervical spinal cord rostral to the injury and neurons in the brain for CST, RST or RtST, respectively. We will count the number of CTB+ neurons in the respective tracts to quantify the spared dPSTs and dLSTs including CST, RST and RtST after graded cervical SCI. Additionally, we have established the method

to anterogradely label different LDTs by AAVs expressing different fluorescence proteins and BDA in normal animals and in animals after hemicontusion (Figure 12, 13). We will use this approach to further confirm the loss of LDTs after graded SCI. We will also examine the projections of these LDTs in the cervical spinal cord and its relationship with dPST neurons in the normal or graded SCI animal. We will carefully analyze the potential correlation between anatomical and functional deficits to understand the roles of dPSTs and/or LDTs in functional deficits after cervical SCI. These data will provide invaluable information to develop new hypotheses for future studies and help to identify the therapeutic target for specific forelimb functional recovery after cervical SCI.

(CTB) was injected in uninjured control at cervical level 7 (C7). Representative images of CTB immunostaining (white) in control animals at C3 rostral (B) and approximately thoracic 1 (T1) caudal (C) to the injection. High magnification images capturing marked neurons (white) in the dorsal (d) and ventral (v) horns on the ipsilateral (left) and contralateral (right) sides. Scale bar = 200 μ m for main images; High magnification images scale bar = 50 μ m. **License for (Figure 10.A):** Title: The Location of the Major Ascending and Descending Spinal Cord Tracts in all Spinal Cord Segments in the Mouse: Actual and Extrapolated; Author: Megan Harrison, Charles Watson; Publication: The Anatomical Record: Advances in Integrative Anatomy and Evolutionary Biology; Publisher: John Wiley and Sons; Date: July 31, 2012; Copyright © 1999 John Wiley & Sons, Inc. License number 4873070881628 granted to Chrystine Gallegos on July 20, 2020. Watson C, Harrison M (2012) The location of the major ascending and descending spinal cord tracts in all spinal cord segments in the mouse: actual and extrapolated. The Anatomical Record: Advances in Integrative Anatomy and Evolutionary Biology 295:1692-1697.

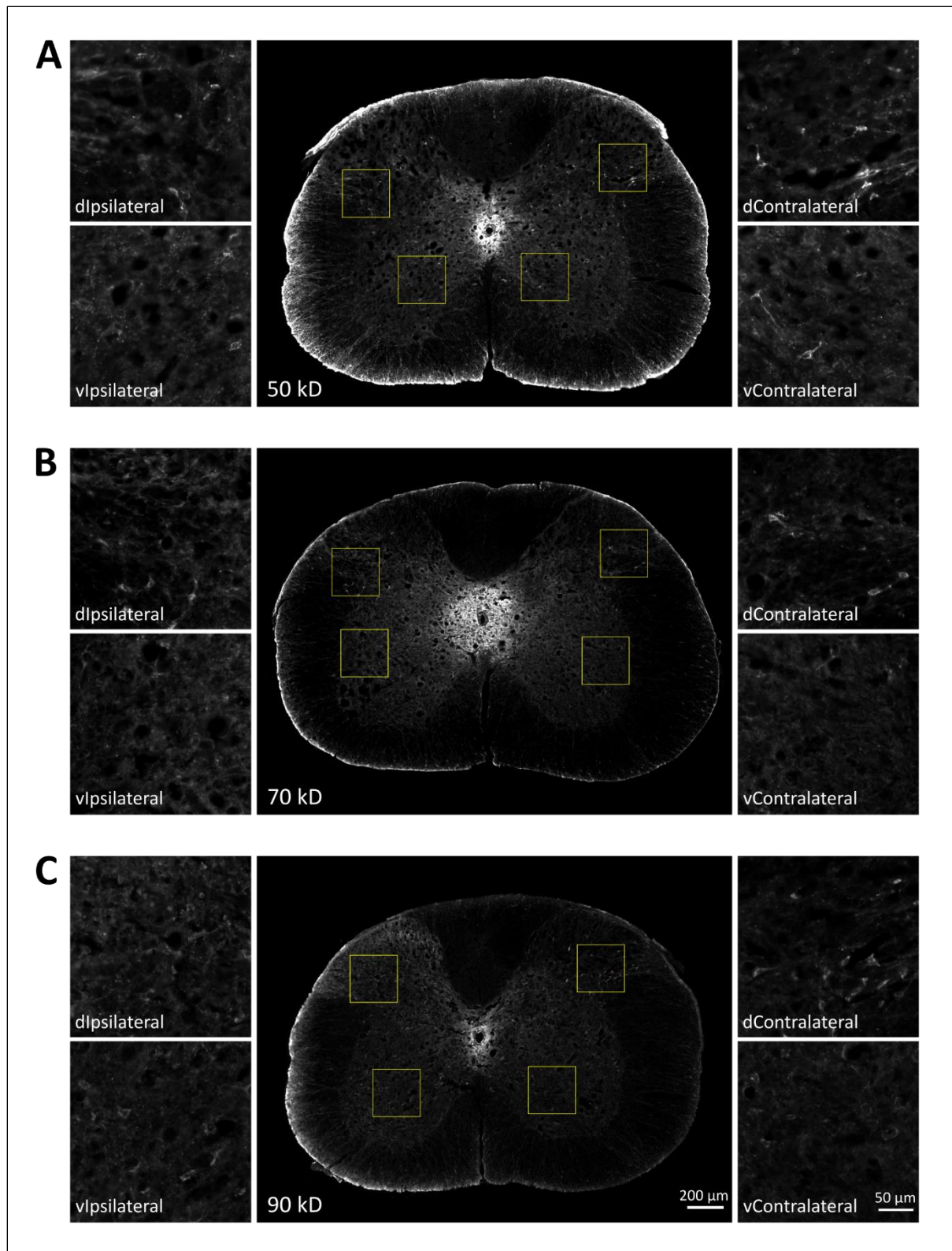


Figure 11 | Validation of spinal CTB retrograde tracing in grade SCI animals. Mice received different severities of hemicontusion injuries of either 50 kD (A), 70 kD (B), or 90 kD (C) at cervical 5 (C5). At 9

weeks post-injury (PI), CTB was injected at C7 caudal to the SCI and animals were sacrificed at 11-12 weeks PI. Representative images of spinal cord cross-sections at C3 demonstrate CTB marked neurons in the dorsal (d) and ventral (v) horns on the ipsilateral (left) and contralateral (right) sides. High magnification images demonstrate CTB immunoreactivity. Scale bar = 200 um for main images; High magnification images scale bar = 50 um.

Rostral Anterograde Tracing

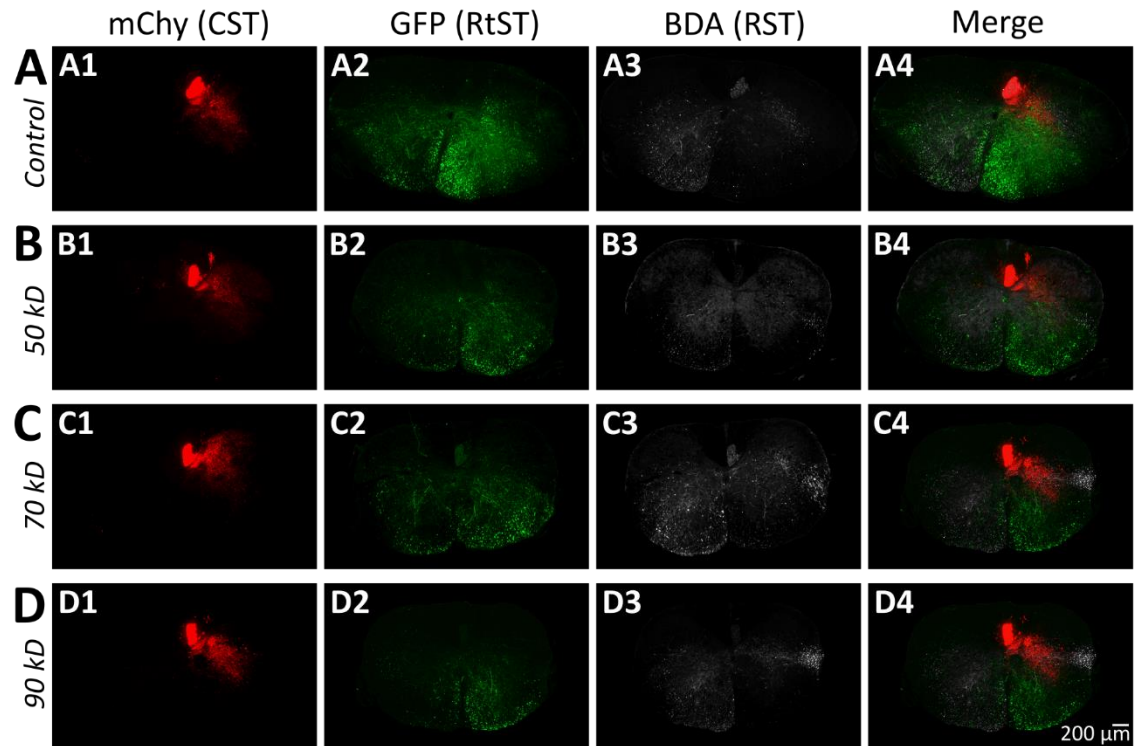


Figure 12 | Rostral cross-sections of spinal descending long tracts by anterograde tracing. AAV5-CAG-mChy was injected into the contralateral motor cortex targeting the corticospinal tract (CST) in control (A1), 50kD (B1), 70kD (C1), and 90kD (D1) groups. The CST can be seen dorsomedially to the central canal. AAV5-CAG-GFP was injected into the ipsilateral pontine reticular nucleus targeting the reticulospinal tract (RtST) in control (A2), 50kD (B3), 70kD (C3), and 90kD (D3) groups. The RtST can be seen in the white matter ventrally to the central canal. Biotinylated dextrin amine was injected into the contralateral red nucleus targeting the rubrospinal tract (RST) in control (A3), 50kD (B3), 70kD (C3), and 90kD (D3) groups. The RST can be seen in the anterior white matter dorsolateral to the dorsal horn in control (A4), 50kD (B4), 70kD (C4), and 90kD (D4) groups. Scale bar = 200um.

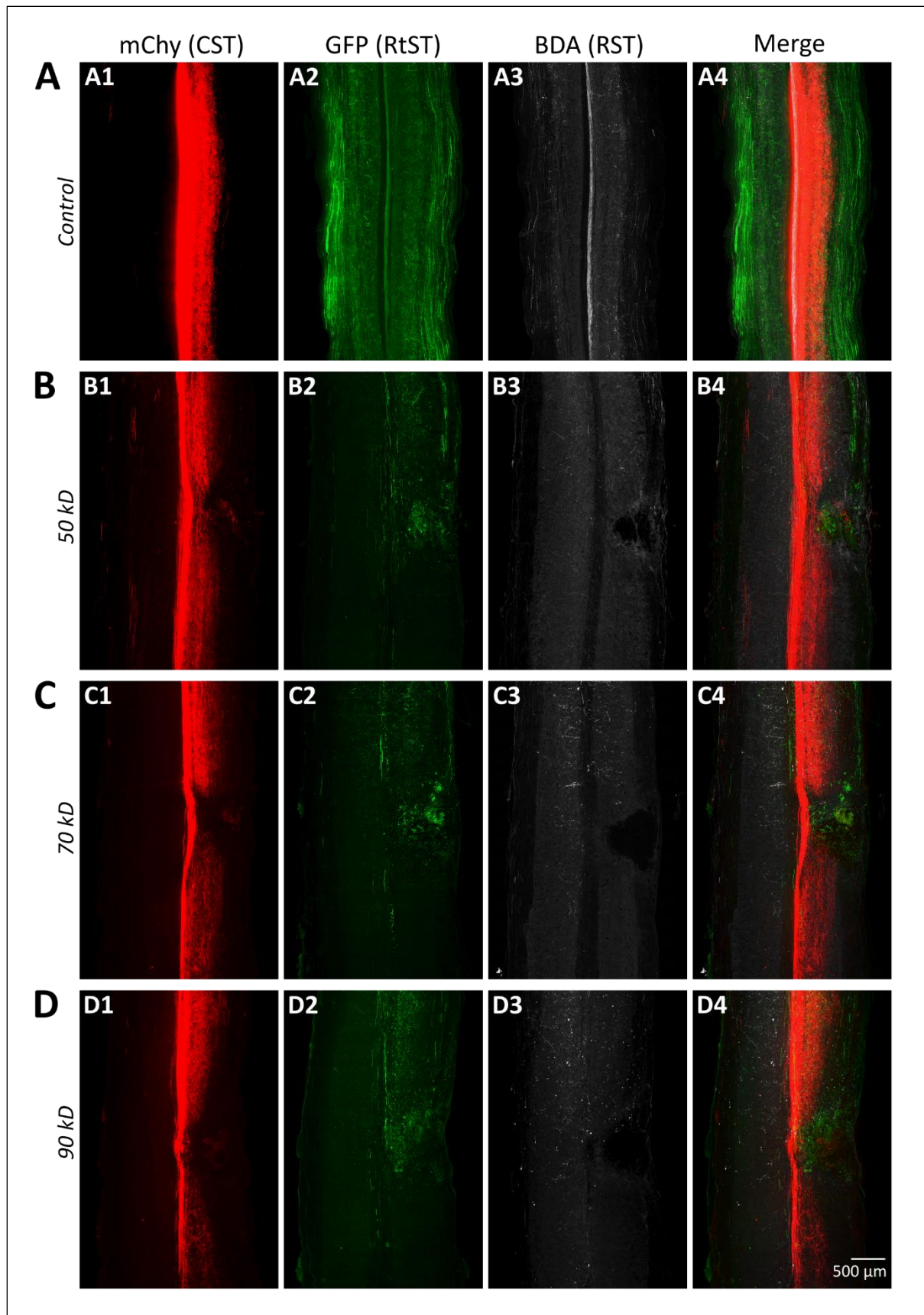


Figure 13 | Longitudinal sections of spinal descending long tracts by anterograde tracing. AAV5-CAG-mch was injected into the contralateral motor cortex targeting the corticospinal tract (CST, red); AAV5-CAG-GFP was injected into the ipsilateral pontine reticular nucleus targeting the reticulospinal tract (RtST, green); and biotinylated dextrin amine (BDA) was injected into the contralateral red nucleus targeting the rubrospinal tract (RST, white) in control animals (A) and in 50kD (B), 70kD (C), and 90kD (D) experimental animals. Representative images show anterograde tracing in control and experimental groups for the CST (A1, B1, C1, D1), RtST (A2, B2, C2, D2), RST (A3, B3, C3, D3), and merged tracts (A4, B4, C4, D4). Images are oriented rostrally (top) to caudally (bottom) for every image. Scale bar = 500um.

Correlations between histology analysis and functional performance

To assess the more nuanced effects of graded SCI on histology and behavioral tests, comparisons were performed to assess the relationship between injury severity, functional performance over time and separately at 9 weeks PI, fibronectin area, and MAP2 volume lost (Figures 14, 15, and 16).

Injury severity showed a strong correlation with MAP2 volume lost ($r_p = 0.85$, $p = 0.0005$) and fibronectin area ($r_p = 0.90$, $p = 0.00002$), confirming the direct effect of injury severity on gray matter loss and injury size. There was also a strong positive correlation between MAP2 volume lost and fibronectin area ($r_p = 0.80$, $p = 0.0019$), demonstrating the relationship between injury size and the effect on gray matter lost. This shows that the injury model worked at performing different severities of SCI that could be assessed histologically.

There was not a relationship between cHL performance over time and fibronectin area or MAP2 lost. However, at 9 weeks PI the percent missteps of cHL had a moderate relationship to injury severity ($r_p = 0.66$, $p = 0.0104$) and fibronectin area ($r_p = 0.65$, $p = 0.0112$). This suggests that greater tissue loss by fibronectin-IR area relates more missteps in cHL (Figure 14).

The performance in rotarod over time was moderately correlated to injury severity ($r_p = -0.65$, $p = 0.0127$) and the area of fibronectin ($r_p = -0.69$, $p = 0.0060$). At 9 weeks PI, rotarod performance had a moderate correlation to injury severity ($r_p = -0.77$, $p = 0.0013$) and MAP2 volume lost ($r_p = -0.67$, $p = 0.0180$), and a strong correlation to fibronectin area ($r_p = -0.89$, $p = 0.00002$). This demonstrates that injury severity and fibronectin area may affect rotarod performance over time, but at 9 weeks PI both gray matter loss and injury size negatively affect performance (Figure 15).

Grooming score over time did not have any correlations with histological outcomes. However, grooming score at 9 weeks PI had a moderate correlation with injury severity ($r_p = -0.64$, $p = 0.0145$), fibronectin area ($r_p = -0.61$, $p = 0.0214$), and MAP2 volume lost ($r_p = -0.78$, $p = 0.0030$). This suggests

that while grooming score measured over time did not associate histologically, when grooming score is correlated at 9 weeks PI injury size and gray matter loss negatively influence performance (Figure 16).

These correlative results demonstrate the grooming is not efficient at detecting nuanced deficits between different injury severities. Instead, complex horizontal ladder and rotarod reflected sensitivity to functional deficit and correlated well with histological outcomes at 9wPI.

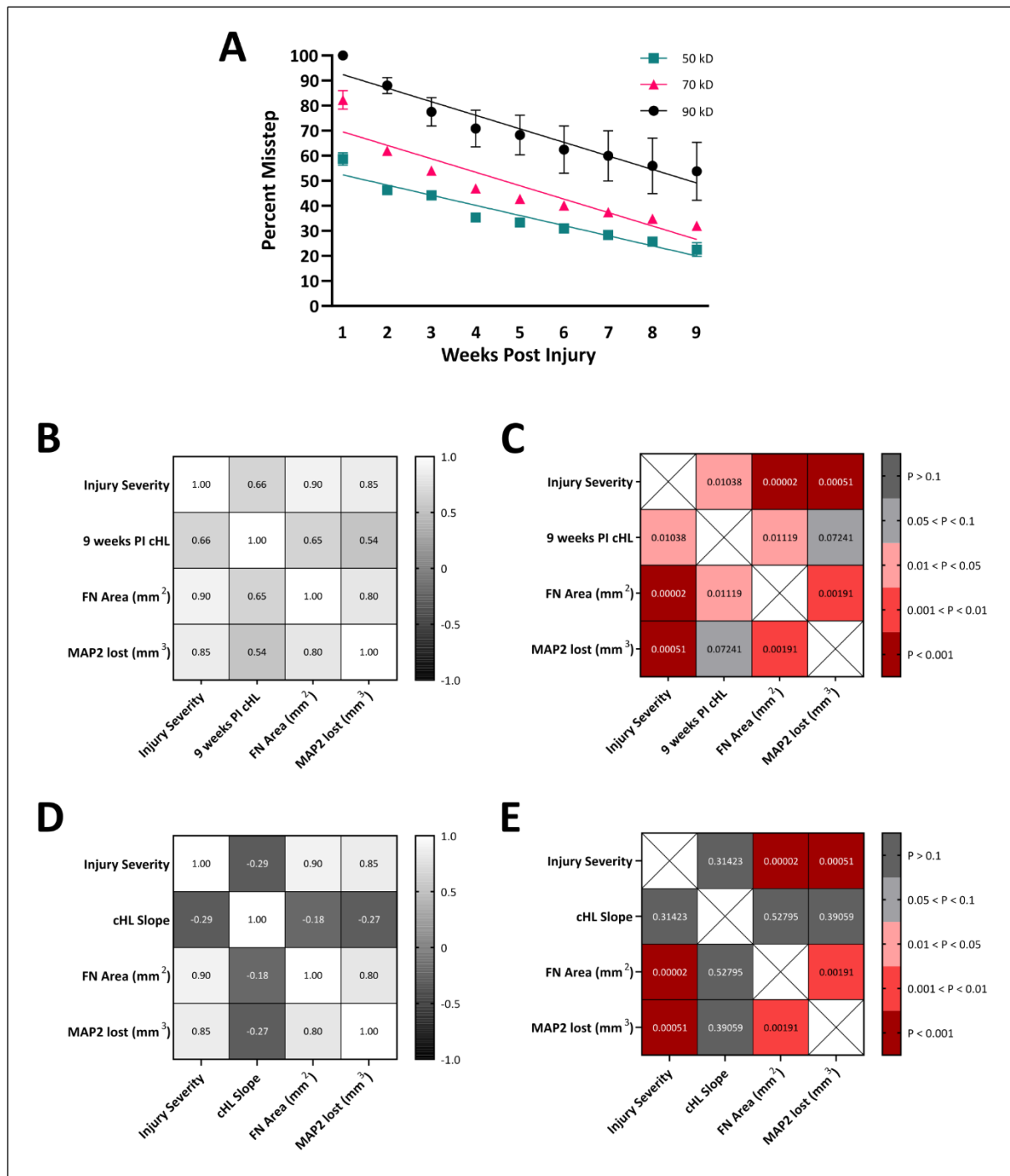


Figure 14 | Relationships between histology and complex horizontal ladder. Linear regression for percent missteps in 50, 70, and 90kD groups (A). Pearson correlational R values (B, D) and p-values (C, E) for scores at 9 weeks PI and the slope rate of change across time.

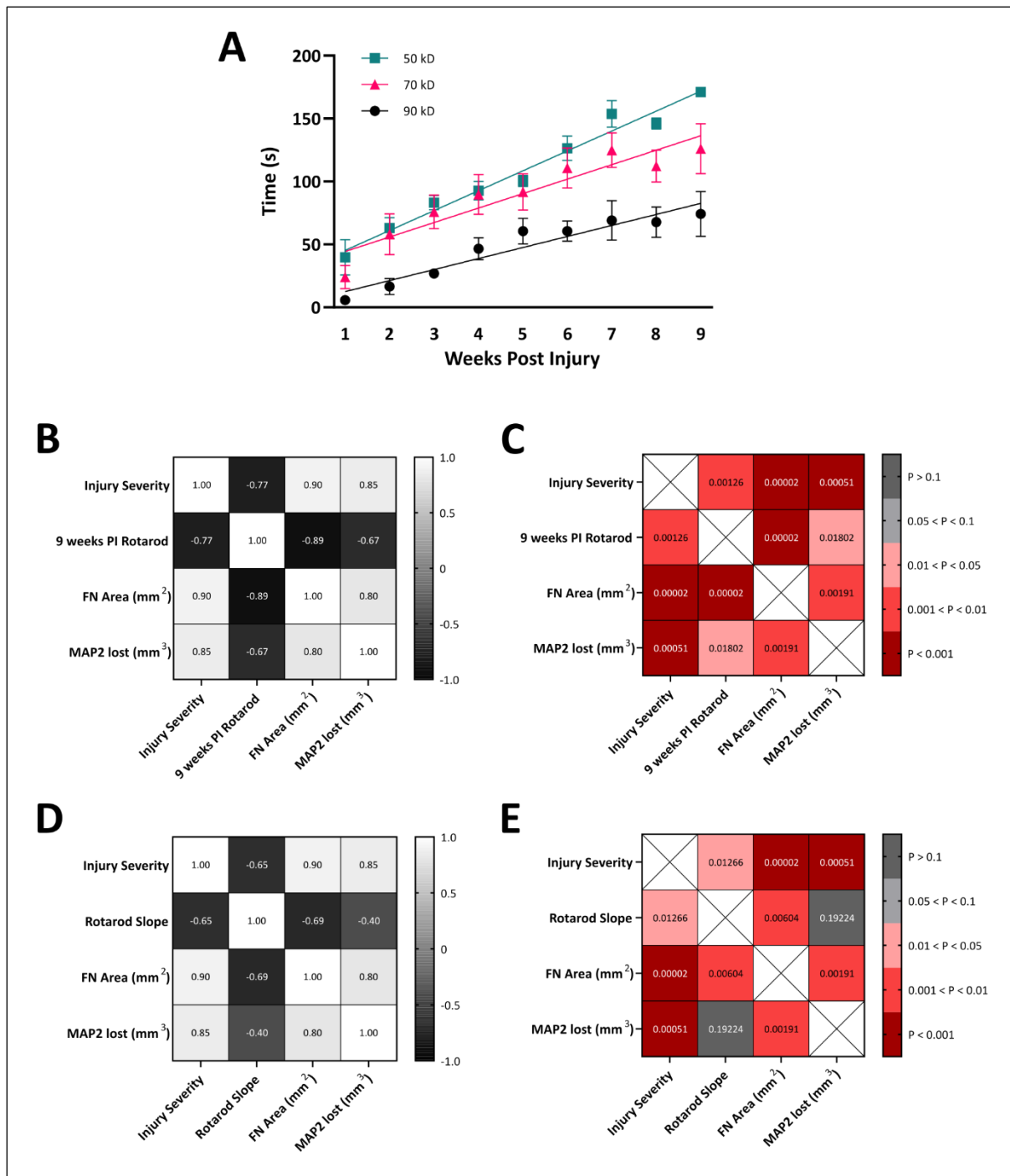


Figure 15 | Relationships between histology and rotarod score. Linear regression for percent missteps in 50, 70, and 90kD groups (A). Pearson correlational R values (B, D) and p-values (C, E) for scores at 9 weeks PI and the slope rate of change across time.

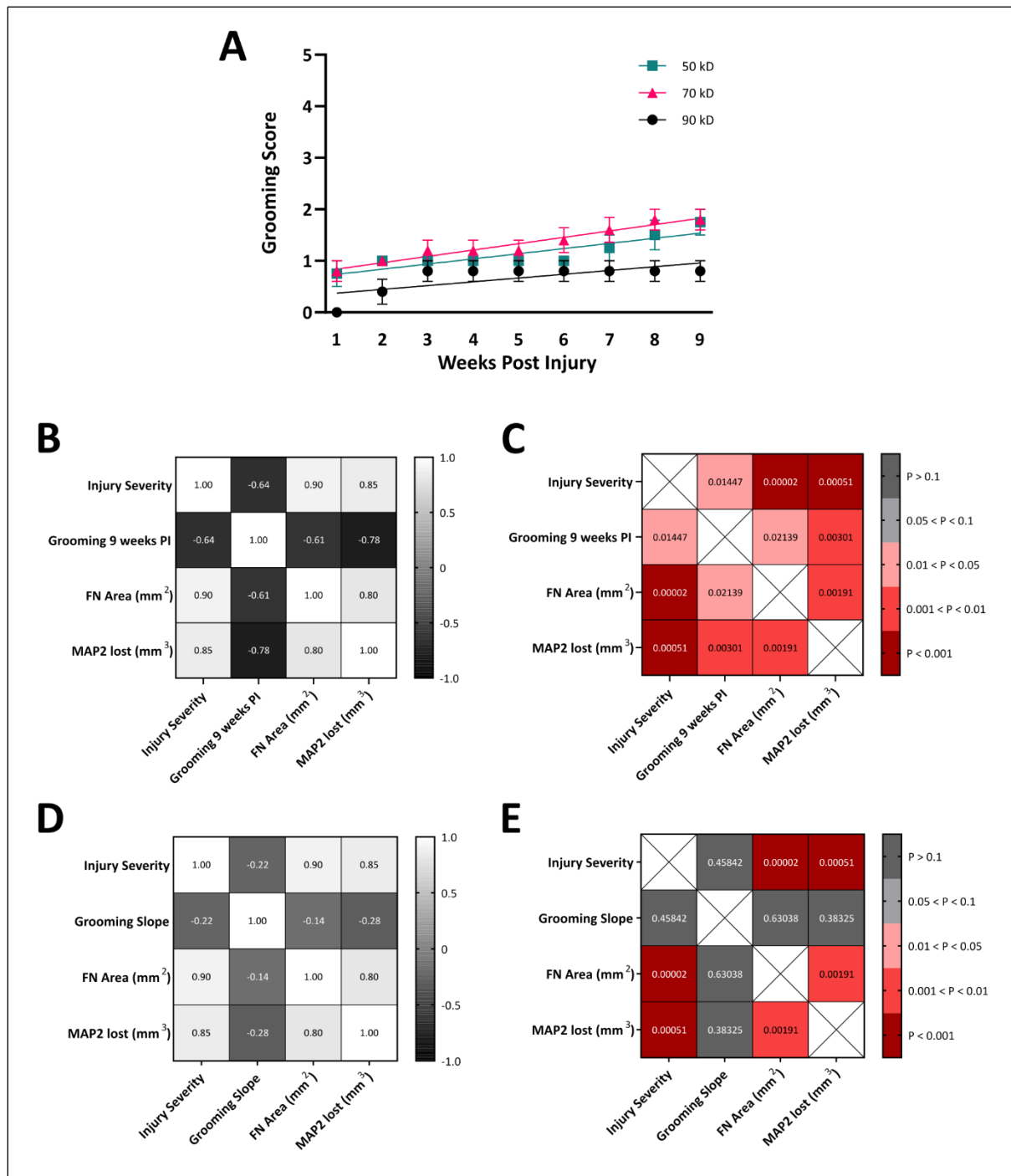


Figure 16 | Relationships between histology and grooming score. Linear regression for percent missteps in 50, 70, and 90kD groups (A). Pearson correlational R values (B, D) and p-values (C, E) for scores at 9 weeks PI and the slope rate of change across time.

Chapter 4 – DISCUSSION

Clinically-relevant cervical hemicontusion graded model

The majority of SCI patients have cervical injuries (54.5%; (Center., 2019) and clinically relevant cervical SCI animal models are critically needed to develop effective treatment for these patients. In this study, we created graded severities of cervical SCI contusions by using different impact forces and then characterized the functional and histological deficits. Our results show that the graded cervical SCI contusions produced histological damage unilaterally and specific forelimb functional deficits on the contusion side; these effects are closely related to injury severity.

This model is a valid representation of repeatable graded cervical SCIs and is more clinically relevant than other laceration/transection, compression, or pinch models. Laceration and transection models are injuries most commonly performed by cutting the dorsal funiculus, partial quadrant or total hemisections, or complete transections; in all of these injuries, any axonal connections caudal to the lesion are totally severed (Geissler et al., 2013). Laceration models are very valuable for assessing axonal regeneration and sprouting as the injuries can be incredibly tract specific, however, these models are not clinically relevant (Aguilar and Steward, 2010; Geissler et al., 2013; Fink and Cafferty, 2016). Compression models are helpful to assess transient stenosis of the spinal canal during the compression and also because this model is first a contusion followed by the prolonged compression (Geissler et al., 2013; Sharif-Alhoseini et al., 2017). These models are good for mimicking the pressure the spinal cord is under during human SCI before surgical intervention can decompress the spinal cord and mimic the ischemic and decompressive environment (Geissler et al., 2013). Pinch and crush models are helpful to assess the inflammatory cascade and reactivity response (Orr et al., 2017) but the effects in functional deficits can be transient (Hilton et al., 2013) which suggests that this model can have a high degree of variability. Furthermore, this model is not representative of human SCI (Geissler et al., 2013). Lacerations and transections are better than contusions at assessing

regeneration and sprouting of specific tracts, while compressions are better to represent the spinal column under pressure before surgery. Pinch models are good for looking at plasticity and the spontaneous recovery response because the effect is not as prolonged as a contusion or hemisection model. Thus, contusions are the best model for representing the human SCI.

Current contusion models initially began using thoracic contusions (Aguilar and Steward, 2010), and have since evolved to using more cervical models that are clinically relevant (Sharif-Alhoseini et al., 2017). While these models are the most clinically accurate, they are also risky due to the proximity to the respiratory tracts (Aguilar and Steward, 2010; Geissler et al., 2013; Sharif-Alhoseini et al., 2017) resulting in the majority of cervical contusions being hemicontusions (Sharif-Alhoseini et al., 2017). Bilateral models previously have shown high mortality rates (Aguilar and Steward, 2010), although a recent successful bilateral mouse contusion did not have high mortality rates (Reinhardt et al., 2020). Even in this study, we had a 20% mortality rate during surgeries. The bilateral model is more clinically relevant than even the hemicontusion model, however, the time cost that goes into training each mouse is high. Using hemicontusion models has successfully represented human SCI very closely, and while rats are the closest model to human SCI to date, mouse SCI offers immense possibility with transgenic options and viral targeting (Aguilar and Steward, 2010).

While there is no true comparable animal model to human cervical SCI, rodent models offer a significant level of manipulability for experimental details such as using tracing mechanisms, the different behavioral assessments, and the ability to process data histologically in a relatively short time frame compared to the human life span. Other studies have assessed compression dwell time to distinguish between injury grades (Streijger et al., 2013; Nishi et al., 2020) rather than contusion force. Previous assessments into the functional deficits after SCI in graded SCI demonstrate that C4 but not C6 injuries produce a chronically reduced response (Hilton et al., 2013), and also performed behavioral assessments examining locomotion and forelimb function overall, but have not assessed

which specific steps are preserved or lost for reaching and grasping (Anderson et al., 2004; Aguilar and Steward, 2010; Streijger et al., 2013; Nishi et al., 2020; Reinhardt et al., 2020). More research into the effects of contusive cervical SCI on the specific steps in reaching and grasping is needed because even partial recovery of function can significantly improve the quality of life for a patient with SCI.

This study uses a clinically relevant injury model, rigorously assesses a series of behavioral tests, and histologically analyzes the anatomical effects of graded SCI. Additionally, it helps to expand the field of knowledge for mouse models using cervical contusions, which is especially important right now with the advent of so many promising tracing and transgenic mouse lines available to further elucidate mechanisms of neuronal injury and recovery (Flynn et al., 2017; Zholudeva et al., 2018).

Functional implications of behavioral tests after graded cervical SCI

Cervical unilateral contusion of different severities sufficiently produced different forelimb functional deficits in animals receiving injuries of 50, 70, or 90kD contusion forces. These deficits are different to deficits observed in thoracic and lumbar spinal mice and rats, as these injuries in rodents affect the hindlimbs (Cao et al., 2005; Nishi et al., 2007; Ichiyama et al., 2008; Wen et al., 2015). The cervical SCI contusion used in this model produced deficits, restricted to the forelimb, consistent with other mouse models (Anderson et al., 2004; Streijger et al., 2013). We used several behavioral tests: complex horizontal ladder, rotarod, grooming, pasta handling, and pellet reaching. We found that the different behavioral tests reflected a level of sensitivity previously unexplored in other cervical mouse studies. The complex horizontal ladder and rotarod tests were sensitive at detecting deficits in different injury severities, while the grooming test was not sensitive to the graded cervical deficits. While the grooming test is a well-established assay to detect sensorimotor deficit in the forelimb, these results suggest that grooming is not sufficient to measure functional changes after cervical contusion SCI in the mouse. This may be because mice also use their feet sometimes to groom if they

cannot reach the area with their forepaw. Following SCI, forelimb function is impaired so cleaning ability by forepaw is reduced because they are not able to reach as far up their head, lowering the score.

In the rotarod assay, our results showed that graded SCI results in forelimb functional deficits in all groups during the first couple of weeks after SCI, although over the nine weeks PI all groups showed a level of recovery. In contrast, the complex horizontal ladder may be better at measuring functional recovery changes over a longer period of time and with more sensitivity than rotarod. The rotarod performance plateaus at 5wPI while the cHL continues improving such that the 70kd never hit a performance plateau during our study. Further research should be done to assess the behavioral plateaus of different injury severities in different behavioral tests, as this will provide more information for functional analysis parameters for other studies. The disparity in the performance plateau between the cHL and rotarod may be due to the rotarod's reliable design with the rod staying in the same place albeit at a changing speed. The irregularly spaced cHL is specifically designed to prevent memorization and reduce motor learning. This encourages active sensorimotor participation in a way more similar to "skilled reaching" rather than "walking", as the mouse specifically has to feel for each rung across the platform. Rotarod does not offer this dynamic performance and relies only off an increase in speed, which mice can adapt to over time (Stanley et al., 2005; Farr et al., 2006) or develop compensatory strategies in the uninjured side (Nishi et al., 2020). The complex ladder stays irregular on purpose, to prevent learning or adaptive mechanisms. This suggests that the cHL may be a better test for assessing skilled forepaw function in the mouse, although it is still prudent to perform other assays such as the rotarod test as the rotarod is well established to detect locomotor difficulty.

While other studies typically employ cylinder testing to assess asymmetry after unilateral SCI (Nishi et al., 2020) or paw preference (Bulman-Fleming et al., 1997), we chose not to use this test because our preliminary studies showed that mice do not rear in a manner that requires forepaw support and

are perfectly comfortable to sit on their haunches for minutes at a time. Instead, we evaluated paw preference and the fine forelimb function of reaching and grasping by pasta handling and the single pellet reaching test. Our results show that pasta handling and pellet reaching are unsatisfactory measures for forelimb function after unilateral cervical SCI contusion. Pasta handling requires either head fixation (Whishaw et al., 2017) or should be set up in a similar chamber as the pellet reaching for it to work, as without any external restrictions mice will instead use their contralateral paw or mouth to engage the pasta pieces. For pellet reaching, we found that if pellets were directly aligned with the chamber opening, mice would use their preferred paw during training but after SCI resorted to their contralateral limb again. This demonstrates that mice are extremely adaptable to adverse situations with their forelimb. In a later study, we found that even if the pellet holder was offset from the reaching chamber opening forcing the mouse to use only their preferred side, mice were still unable to reach simply because the functional loss was too severe after SCI.

We would suggest using the Modified Montoya Staircase to supplement single pellet reaching, which has been used successfully in this lab in rat cervical hemicontusion models (Gallegos et al., 2020). Using the Modified Montoya Staircase as a supplementary assessment could provide more parameters to assess the mouse on and also might allow for some quantification details due to the sensitivity of color coding pellets and different step levels. The step levels allow an assessment for range of motion, the number of pellets taken/displaced/lost allow for a measure of reaching ability, and the pellets eaten serves as a measure of grasping ability and accuracy rate. It would be worthwhile to research more than one forelimb functional assay in a graded SCI and assess the behavioral functions lost or preserved between groups as well as performance plateaus over time.

Histology deficits after graded SCI

Our model produced an injury with scar formation in the injury center with a glial border and a fibrotic core. This is consistent with other mouse SCI models which also found lesions filled in with fibronectin surrounded by reactive astrocytes (Cooper et al., 2018; Nishi et al., 2020). Importantly, fibronectin indicates the lesion size and correlates with injury severity and gray matter loss, demonstrating that gray matter and white matter are damaged after injury and that the damage continues chronically in the secondary injury response. Reducing the inhibitory environment will be very important for promoting regeneration or sprouting of propriospinal axons or increasing the plasticity of nearby tracts that could be important for forming spinal detours around lesions.

Gray matter volume was significantly impacted by injury severity, as is consistent with other SCI models assessing the gray matter volume (Streijger et al., 2013) and the fact that SCI affects the white and gray matter of the spinal cord (Reinhardt et al., 2020). Since the axon tracts for both descending cortical and propriospinal axons are in the white matter, it's important to further elucidate the mechanisms of functional deficit to develop treatment for patients. This first starts by understanding the relationship functional testing has to histological outcomes as in this study, and, importantly, deeply assessing the preservation or loss of the 10 specific steps involved in a reach and grasp (Metz and Whishaw, 2002). By uncovering the mechanism of SCI functional deficit, we can work towards identifying therapeutic targets and creating treatments. By discovering which specific steps in reaching and grasping are affected by dLSTs versus dPSTs or the combination of both, we can explore potentials for detour circuits either by endogenous plasticity or by promoting plasticity through treatments. Taken together, the mechanism of functional deficits and the tract specific contributions will be vital to designing an effective treatment for SCI patients.

We assessed the differences in gray matter loss by MAP2 volume and injury size by fibronectin area between the different injury grades. Our fibronectin quantification results confirmed that a

greater contusion force would produce a more severe SCI. This is consistent with previous studies demonstrating that increasing compression time is correlated to gray matter (Streijger et al., 2013) or MAP2 loss and injury severity, but there were no significant differences between the 50 and 70kD groups for gray matter volume lost. This is on par with assessing white matter loss between injury grades after 30kD contusion using varying dwell times for severities, which also found that there were no significant differences between the dwell times in this mild injury (Nishi et al., 2020).

Interestingly, we found differences in the shape of the fibrotic scar between all injury grades. We observed that the 90kD group showed a lesion that extended more rostrally and caudally while the 50 and 70kD groups maintained a spherical shape. The cavity was filled in for all injury groups as expected (Zhu et al., 2015; Cooper et al., 2018) and displayed the characteristic chronic scar.

The relationship between histology and functional deficits

We wanted to see the relationships between functional performance and histological outcome between injury grades. We used fibronectin to assess injury size and MAP2 to look at gray matter loss. In the future, we will use CTB to assess the potential roles of dPSTs in forelimb functional deficit after SCI.

After SCI, lesion areas are filled with fibronectin and an astroglial border surrounds the injury to contain it (Tran et al., 2018). Fibronectin is a very reliable marker in mice of the lesion size (Zhu et al., 2015). Typically the infiltration of fibronectin is assessed in hemisection, transection, or dorsal column laceration models as fibroblasts are thought to migrate with infiltrating pericytes after the dura of the spinal cord injury is broken during injury (Zhu et al., 2015; Cooper et al., 2018; Tran et al., 2018). Assessing fibronectin is important as fibrosis is a major barrier to axonal growth and could secrete factors recruiting other inflammatory molecules or inhibitory agents into the area (Silva et al., 2014; Tran et al., 2018).

In terms of the impact of gray matter damage to function deficits, there were no relationships found between MAP2 lost volume and cHL, rotarod, or grooming performance over time. MAP2 was able to predict rotarod and grooming performance but not cHL at 9 weeks PI, which implies that gray matter damage did not affect the rate of change of recovery during the weeks PI. This is interesting because previous studies suggest that neuronal loss is correlated to the functional deficits (Nishi et al., 2020), but this study demonstrates that neuronal loss might not impact function as much as white matter damage. Previous studies assessing ablation and tract specific damage indicate that gray matter damage may play a more significant role in spontaneous recovery or some level of gray matter remodeling by plasticity rather than long term functional improvements (Fink and Cafferty, 2016).

We wanted to assess the correlation between injury severity and gray matter loss with the functional deficit, hypothesizing that different injury severity would have a different functional deficit. When we looked at the rate of change over time for each group, we found that only fibronectin was able to predict rotarod performance. This implies that while injury size did not influence the rate of change during the first nine weeks for cHL and grooming, it did impact the rotarod performance. We found that MAP2 was unable to predict any behavioral performance in the rate of change over time, which is interesting as typically it's believed that the neuronal loss is a significant cause of the functional deficit after SCI (Nishi et al., 2020). Importantly, only our behavioral data at 9 weeks PI displayed a relationship between injury and functional deficit, which is consistent with other studies using behavior at 8 weeks PI for correlations with histology (Nishi et al., 2020).

Overall, our correlational results suggest that gray matter loss and injury size are much better predictors of functional deficits at the end point of behavior, i.e. 9 weeks PI in this study, but are not good efficient predictors of the rate of change for performance in cHL, rotarod, and grooming across time. Finding a sensitive, specific behavioral test for forelimb functional deficit in mice is important, as currently in our study and in previous studies, mice are adaptive and develop compensatory

strategies post-injury (Stanley et al., 2005; Farr et al., 2006). Importantly, our results in gray matter loss by MAP2 demonstrate that different injury severities have different volumes of gray matter damage. In the future, we hope to explore the deeper relationships in communication damage by assessing white matter damage in dPSTs and dLSTs. It is likely that different injury severities comparably result in different amounts of white matter damage, so a graded SCI contusion model as in this study shows the potential of using clinically relevant cervical contusion models to sensitively detect the different anatomical and functional deficits between injury severities.

Potential roles of descending spinal tracts after cervical SCI

In this study, we have assessed the effects of graded SCI on injury size, gray matter loss, and behavioral deficits in the preferred forelimb after cervical hemicontusion. We next plan to use a retrograde tracing approach to quantify the number of descending propriospinal neurons rostral to the injury that project to cervical spinal cord segments caudal to the injury. We will be using cholera toxin subunit B (CTB) as a retrograde tracer and counting the neurons at C4 and C3, which are short propriospinal interneurons (PINs) as they connect close cervical segments, in contrast to long PINs connecting distant cervical and lumbar segments. Long tract PINs are implicated in coordination, central pattern generation, and forming locomotor detour circuits (Zholudeva et al., 2018), while the shorter tract PINs may be more implicated in task specific function such as fine skilled reaching and grasping. Recovering this ability is very important to patients with cervical SCI as it offers a significant level of independence and improved quality of life. The spinal cord neurons including dPST neurons play important roles in normal locomotion and functional recovery after SCI. PINs perform a variety of functions including modulating supraspinal and sensory signals as well as coordinating motor output (Flynn et al., 2017; Zholudeva et al., 2018; Laliberte et al., 2019; Zavvarian et al., 2020). Additionally, spared PINs in cervical spinal cord rostral to the injury could serve as neuronal relays for

detour circuits reconnecting the injured LDTs and their targeted spinal neurons below the injury. Newly formed detour circuits through PINs could play important roles in functional recovery after SCI, although more research is needed.

Future directions and Conclusion

In the future, we will assess CTB retrograde tracing and AAV and BDA anterograde tracing to analyze neuronal connections between propriospinal and long distances, respectively. We significantly need to find a behavioral test that is sensitive to forelimb functional deficits after SCI specifically in the reaching and grasping parameters. Currently, we have not found one that allows a deep analysis into which functions of the reaching and grasping steps are preserved. Discovering which functions are preserved and the anatomical correlates will help us develop targeted therapies to promote repair and regeneration after SCI. We will also use chemogenetics to turn propriospinal interneurons on and off and assess the impacts on functional recovery and deficits in normal animals and after graded SCI.

Our study demonstrated the effects of graded cervical hemicontusion in mice in terms of functional deficits and anatomical correlates. We have explored the sensitivity of different behavioral test and observed that rotarod and cHL display the most promise in detecting subtle differences between injury grades. Our histological assessment confirmed our hypothesis that injury size and gray matter loss would be impacted by injury severity. We have also confirmed our hypothesis that different injury severity results in different functional deficits, but we would further like to assess the difference in reaching and grasping functional deficits specifically. This study demonstrates the differences in function and histology after graded SCI and provides a baseline for further studies assessing the extent of tract involvement and the role of descending propriospinal tracts after SCI.

BIBLIOGRAPHY

- Aguilar RM, Steward O (2010) A bilateral cervical contusion injury model in mice: assessment of gripping strength as a measure of forelimb motor function. *Experimental neurology* 221:38-53.
- Ahmed RU, Alam M, Zheng Y-P (2019) Experimental spinal cord injury and behavioral tests in laboratory rats. *Heliyon* 5:e01324.
- Allred RP, Adkins DL, Woodlee MT, Husbands LC, Maldonado MA, Kane JR, Schallert T, Jones TA (2008) The vermicelli handling test: a simple quantitative measure of dexterous forepaw function in rats. *Journal of neuroscience methods* 170:229-244.
- Anderson KD, Abdul M, Steward O (2004) Quantitative assessment of deficits and recovery of forelimb motor function after cervical spinal cord injury in mice. *Experimental neurology* 190:184-191.
- Anderson KD, Gunawan A, Steward O (2005) Quantitative assessment of forelimb motor function after cervical spinal cord injury in rats: relationship to the corticospinal tract. *Experimental neurology* 194:161-174.
- Anderson MA, O'Shea TM, Burda JE, Ao Y, Barlatey SL, Bernstein AM, Kim JH, James ND, Rogers A, Kato B (2018) Required growth facilitators propel axon regeneration across complete spinal cord injury. *Nature* 561:396-400.
- Armour BS, Courtney-Long EA, Fox MH, Fredine H, Cahill A (2016) Prevalence and causes of paralysis—United States, 2013. *American journal of public health* 106:1855-1857.
- Atasoy D, Sternson SM (2018) Chemogenetic tools for causal cellular and neuronal biology. *Physiological Reviews* 98:391-418.
- Bertelli JA, Mira J-C (1993) Behavioral evaluating methods in the objective clinical assessment of motor function after experimental brachial plexus reconstruction in the rat. *Journal of neuroscience methods* 46:203-208.

- Bulman-Fleming MB, Bryden MP, Rogers TT (1997) Mouse paw preference: effects of variations in testing protocol. *Behavioural brain research* 86:79-87.
- Cao Q, Zhang YP, Iannotti C, DeVries WH, Xu XM, Shields CB, Whittemore SR (2005) Functional and electrophysiological changes after graded traumatic spinal cord injury in adult rat. *Exp Neurol* 191 Suppl 1:S3-S16.
- Center NSCIS (2019) Facts and Figures at a Glance. . In. Birmingham, AL: University of Alabama at Birmingham.
- Center. NSCIS (2019) 2019 Annual Statistical Report for the Spinal Cord Injury Model Systems. In. Birmingham, Alabama: University of Alabama at Birmingham.
- Chen K, Deng S, Lu H, Zheng Y, Yang G, Kim D, Cao Q, Wu JQ (2013) RNA-seq characterization of spinal cord injury transcriptome in acute/subacute phases: a resource for understanding the pathology at the systems level. *PloS one* 8:e72567.
- Cherian T, Ryan D, Weinreb J, Cherian J, Paul J, Lafage V, Kirsch T, Errico T (2014) Spinal cord injury models: a review. *Spinal cord* 52:588-595.
- Chhaya SJ, Quiros-Molina D, Tamashiro-Orrego AD, Houle JD, Detloff MR (2019) Exercise-Induced Changes to the Macrophage Response in the Dorsal Root Ganglia Prevent Neuropathic Pain after Spinal Cord Injury. *J Neurotrauma* 36:877-890.
- Cooper JG, Jeong SJ, McGuire TL, Sharma S, Wang W, Bhattacharyya S, Varga J, Kessler JA (2018) Fibronectin EDA forms the chronic fibrotic scar after contusive spinal cord injury. *Neurobiol Dis* 116:60-68.
- Dai H, MacArthur L, McAtee M, Hockenbury N, Das P, Bregman BS (2011) Delayed rehabilitation with task-specific therapies improves forelimb function after a cervical spinal cord injury. *Restorative neurology and neuroscience* 29:91-103.

- DeVivo MJ, Chen Y (2011) Trends in new injuries, prevalent cases, and aging with spinal cord injury. *Archives of physical medicine and rehabilitation* 92:332-338.
- Dunham KA, Siriphorn A, Chompoopong S, Floyd CL (2010) Characterization of a graded cervical hemicontusion spinal cord injury model in adult male rats. *J Neurotrauma* 27:2091-2106.
- Erskine EL, Smaila BD, Plunet W, Liu J, Raffaele EE, Tetzlaff W, Kramer JL, Ramer MS (2019) Skilled reaching deterioration contralateral to cervical hemicontusion in rats is reversed by pregabalin treatment conditional upon its early administration. *Pain Reports* 4.
- Fakhoury M (2015) Spinal cord injury: overview of experimental approaches used to restore locomotor activity. *Reviews in the Neurosciences* 26:397-405.
- Fan C, Zheng Y, Cheng X, Qi X, Bu P, Luo X, Kim DH, Cao Q (2013) Transplantation of D15A-expressing glial-restricted-precursor-derived astrocytes improves anatomical and locomotor recovery after spinal cord injury. *International journal of biological sciences* 9:78.
- Farr TD, Whishaw IQ (2002) Quantitative and qualitative impairments in skilled reaching in the mouse (*Mus musculus*) after a focal motor cortex stroke. *Stroke* 33:1869-1875.
- Farr TD, Liu L, Colwell KL, Whishaw IQ, Metz GA (2006) Bilateral alteration in stepping pattern after unilateral motor cortex injury: a new test strategy for analysis of skilled limb movements in neurological mouse models. *Journal of neuroscience methods* 153:104-113.
- Fink KL, Cafferty WB (2016) Reorganization of intact descending motor circuits to replace lost connections after injury. *Neurotherapeutics* 13:370-381.
- Flynn JR, Conn V, Boyle KA, Hughes DI, Watanabe M, Velasquez T, Goulding MD, Callister RJ, Graham BA (2017) Anatomical and molecular properties of long descending propriospinal neurons in mice. *Frontiers in neuroanatomy* 11:5.
- Gallegos C, Carey M, Zheng Y, He X, Cao QL (2020) Reaching and grasping training improves functional recovery after chronic cervical spinal cord injury. *Frontiers in Cellular Neuroscience* 14.

- Geissler SA, Schmidt CE, Schallert T (2013) Rodent models and behavioral outcomes of cervical spinal cord injury. *Journal of spine*.
- Gensel JC, Tovar CA, Hamers FP, Deibert RJ, Beattie MS, Bresnahan JC (2006) Behavioral and histological characterization of unilateral cervical spinal cord contusion injury in rats. *Journal of neurotrauma* 23:36-54.
- Guo Y, Hu H, Wang J, Zhang M, Chen K (2019) Walking Function After Cervical Contusion and Distraction Spinal Cord Injuries in Rats. *J Exp Neurosci* 13:1179069519869615.
- Haines DE, Mihailoff GA, Yezierski RP (2018) The Spinal Cord. In: *Fundamental Neuroscience for Basic and Clinical Applications*, pp 138-151.e131.
- Hill RL, Zhang YP, Burke DA, DeVries WH, Zhang Y, Magnuson DS, Whittemore SR, Shields CB (2009) Anatomical and functional outcomes following a precise, graded, dorsal laceration spinal cord injury in C57BL/6 mice. *Journal of neurotrauma* 26:1-15.
- Hilton BJ, Assinck P, Duncan GJ, Lu D, Lo S, Tetzlaff W (2013) Dorsolateral funiculus lesioning of the mouse cervical spinal cord at C4 but not at C6 results in sustained forelimb motor deficits. *Journal of neurotrauma* 30:1070-1083.
- Houle JD, Tom VJ, Mayes D, Wagoner G, Phillips N, Silver J (2006) Combining an autologous peripheral nervous system “bridge” and matrix modification by chondroitinase allows robust, functional regeneration beyond a hemisection lesion of the adult rat spinal cord. *Journal of Neuroscience* 26:7405-7415.
- Ichiyama RM, Courtine G, Gerasimenko YP, Yang GJ, van den Brand R, Lavrov IA, Zhong H, Roy RR, Edgerton VR (2008) Step training reinforces specific spinal locomotor circuitry in adult spinal rats. *J Neurosci* 28:7370-7375.

- Jeong SJ, Cooper JG, Ifergan I, McGuire TL, Xu D, Hunter Z, Sharma S, McCarthy D, Miller SD, Kessler JA (2017) Intravenous immune-modifying nanoparticles as a therapy for spinal cord injury in mice. *Neurobiol Dis* 108:73-82.
- Khaing ZZ, Geissler SA, Jiang S, Milman BD, Aguilar SV, Schmidt CE, Schallert T (2012) Assessing forelimb function after unilateral cervical spinal cord injury: novel forelimb tasks predict lesion severity and recovery. *Journal of neurotrauma* 29:488-498.
- Ko H-Y (2019) Biomechanics and Pathophysiology of Spinal Cord Injuries. In: *Management and Rehabilitation of Spinal Cord Injuries*, pp 73-80.
- Kumamaru H, Lu P, Rosenzweig ES, Kadoya K, Tuszynski MH (2019) Regenerating corticospinal axons innervate phenotypically appropriate neurons within neural stem cell grafts. *Cell reports* 26:2329-2339. e2324.
- Laliberte AM, Goltash S, Lalonde NR, Bui TV (2019) Propriospinal neurons: essential elements of locomotor control in the intact and possibly the injured spinal cord. *Frontiers in Cellular Neuroscience* 13:512.
- Lee JH, Tigchelaar S, Liu J, Stammers AM, Streijger F, Tetzlaff W, Kwon BK (2010) Lack of neuroprotective effects of simvastatin and minocycline in a model of cervical spinal cord injury. *Experimental neurology* 225:219-230.
- Lee JH, Streijger F, Tigchelaar S, Maloon M, Liu J, Tetzlaff W, Kwon BK (2012) A contusive model of unilateral cervical spinal cord injury using the infinite horizon impactor. *JoVE (Journal of Visualized Experiments)*:e3313.
- Lewandowski G, Steward O (2014) AAVshRNA-mediated suppression of PTEN in adult rats in combination with salmon fibrin administration enables regenerative growth of corticospinal axons and enhances recovery of voluntary motor function after cervical spinal cord injury. *Journal of Neuroscience* 34:9951-9962.

- Little JW (2006) Spinal Cord Injury: Promise, Progress, and Priorities. *The Journal of Spinal Cord Medicine* 29:172.
- Lo C, Tran Y, Anderson K, Craig A, Middleton J (2016) Functional priorities in persons with spinal cord injury: using discrete choice experiments to determine preferences. *Journal of neurotrauma* 33:1958-1968.
- Loy K, Bareyre FM (2019) Rehabilitation following spinal cord injury: how animal models can help our understanding of exercise-induced neuroplasticity. *Neural Regen Res* 14:405-412.
- Marquardt LM, Doulames VM, Wang AT, Dubbin K, Suhar RA, Kratochvil MJ, Medress ZA, Plant GW, Heilshorn SC (2020) Designer, injectable gels to prevent transplanted Schwann cell loss during spinal cord injury therapy. *Science advances* 6:eaaz1039.
- Metz GA, Whishaw IQ (2002) Cortical and subcortical lesions impair skilled walking in the ladder rung walking test: a new task to evaluate fore-and hindlimb stepping, placing, and co-ordination. *Journal of neuroscience methods* 115:169-179.
- Metz GA, Whishaw IQ (2009) The ladder rung walking task: a scoring system and its practical application. *JoVE (Journal of Visualized Experiments)*:e1204.
- Mitchell EJ, McCallum S, Dewar D, Maxwell DJ (2016) Corticospinal and reticulospinal contacts on cervical commissural and long descending propriospinal neurons in the adult rat spinal cord; evidence for powerful reticulospinal connections. *PLoS One* 11:e0152094.
- Mondello SE, Sunshine MD, Fishedick AE, Moritz CT, Horner PJ (2015) A cervical hemi-contusion spinal cord injury model for the investigation of novel therapeutics targeting proximal and distal forelimb functional recovery. *Journal of neurotrauma* 32:1994-2007.
- Nishi RA, Badner A, Hooshmand MJ, Creasman DA, Liu H, Anderson AJ (2020) The effects of mouse strain and age on a model of unilateral cervical contusion spinal cord injury. *Plos one* 15:e0234245.

- Nishi RA, Liu H, Chu Y, Hamamura M, Su MY, Nalcioğlu O, Anderson AJ (2007) Behavioral, histological, and ex vivo magnetic resonance imaging assessment of graded contusion spinal cord injury in mice. *J Neurotrauma* 24:674-689.
- Noristani HN, They L, Perrin FE (2018) C57BL/6 and Swiss Webster Mice Display Differences in Mobility, Gliosis, Microcavity Formation and Lesion Volume After Severe Spinal Cord Injury. *Front Cell Neurosci* 12:173.
- Onifer SM, Zhang YP, Burke DA, Brooks DL, Decker JA, McClure NJ, Floyd AR, Hall J, Proffitt BL, Shields CB (2005) Adult rat forelimb dysfunction after dorsal cervical spinal cord injury. *Experimental neurology* 192:25-38.
- Oorschot D (1994) Are you using neuronal densities, synaptic densities or neurochemical densities as your definitive data? There is a better way to go. *Progress in neurobiology* 44:233-247.
- Orr MB, Simkin J, Bailey WM, Kadambi NS, McVicar AL, Veldhorst AK, Gensel JC (2017) Compression decreases anatomical and functional recovery and alters inflammation after contusive spinal cord injury. *Journal of neurotrauma* 34:2342-2352.
- Reinhardt D, Stehlik K, Satkunendrarajah K, Kroner A (2020) Bilateral cervical contusion spinal cord injury: A mouse model to evaluate sensorimotor function. *Experimental neurology*:113381.
- Ruder L, Takeoka A, Arber S (2016) Long-Distance Descending Spinal Neurons Ensure Quadrupedal Locomotor Stability. *Neuron* 92:1063-1078.
- Saliani A, Perraud B, Duval T, Stikov N, Rossignol S, Cohen-Adad J (2017) Axon and myelin morphology in animal and human spinal cord. *Frontiers in neuroanatomy* 11:129.
- Schrimsher GW, Reier PJ (1993) Forelimb motor performance following dorsal column, dorsolateral funiculi, or ventrolateral funiculi lesions of the cervical spinal cord in the rat. *Experimental neurology* 120:264-276.

- Sharif-Alhoseini M, Khormali M, Rezaei M, Safdarian M, Hajighadery A, Khalatbari M, Meknatkhah S, Rezvan M, Chalangari M, Derakhshan P (2017) Animal models of spinal cord injury: a systematic review. *Spinal Cord* 55:714-721.
- Silva NA, Sousa N, Reis RL, Salgado AJ (2014) From basics to clinical: a comprehensive review on spinal cord injury. *Progress in neurobiology* 114:25-57.
- Simpson LA, Eng JJ, Hsieh JT, Wolfe, the Spinal Cord Injury Rehabilitation Evidence Research Team DL (2012) The health and life priorities of individuals with spinal cord injury: a systematic review. *Journal of neurotrauma* 29:1548-1555.
- Singh A, Tetreault L, Kalsi-Ryan S, Nouri A, Fehlings MG (2014) Global prevalence and incidence of traumatic spinal cord injury. *Clinical epidemiology* 6:309.
- Soblosky JS, Song J-H, Dinh DH (2001) Graded unilateral cervical spinal cord injury in the rat: evaluation of forelimb recovery and histological effects. *Behavioural brain research* 119:1-13.
- Soderblom C, Luo X, Blumenthal E, Bray E, Lyapichev K, Ramos J, Krishnan V, Lai-Hsu C, Park KK, Tsoulfas P (2013) Perivascular fibroblasts form the fibrotic scar after contusive spinal cord injury. *Journal of Neuroscience* 33:13882-13887.
- Stanley JL, Lincoln RJ, Brown TA, McDonald LM, Dawson GR, Reynolds DS (2005) The mouse beam walking assay offers improved sensitivity over the mouse rotarod in determining motor coordination deficits induced by benzodiazepines. *Journal of Psychopharmacology* 19:221-227.
- Steward O, Willenberg R (2017) Rodent spinal cord injury models for studies of axon regeneration. *Experimental Neurology* 287:374-383.
- Streijger F, Beernink TM, Lee JH, Bhatnagar T, Park S, Kwon BK, Tetzlaff W (2013) Characterization of a cervical spinal cord hemicontusion injury in mice using the infinite horizon impactor. *Journal of neurotrauma* 30:869-883.

- Tennant KA, Asay AL, Allred RP, Ozburn AR, Kleim JA, Jones TA (2010) The vermicelli and capellini handling tests: simple quantitative measures of dexterous forepaw function in rats and mice. *JoVE (Journal of Visualized Experiments)*:e2076.
- Tran AP, Warren PM, Silver J (2018) The biology of regeneration failure and success after spinal cord injury. *Physiological Reviews* 98:881-917.
- Ueno M, Nakamura Y, Li J, Gu Z, Niehaus J, Maezawa M, Crone SA, Goulding M, Baccei ML, Yoshida Y (2018) Corticospinal Circuits from the Sensory and Motor Cortices Differentially Regulate Skilled Movements through Distinct Spinal Interneurons. *Cell Rep* 23:1286-1300 e1287.
- Wang X, Liu Y, Li X, Zhang Z, Yang H, Zhang Y, Williams PR, Alwahab NSA, Kapur K, Yu B, Zhang Y, Chen M, Ding H, Gerfen CR, Wang KH, He Z (2017) Deconstruction of Corticospinal Circuits for Goal-Directed Motor Skills. *Cell* 171:440-455 e414.
- Warren PM, Awad BI, Gutierrez DV, Hoy KC, Steinmetz MP, Alilain WJ, Gensel JC (2019) Cervical Hemicontusion Spinal Cord Injury Model. In: *Animal Models of Acute Neurological Injury*, pp 431-451: Springer.
- Watson C, Harrison M (2012) The location of the major ascending and descending spinal cord tracts in all spinal cord segments in the mouse: actual and extrapolated. *The Anatomical Record: Advances in Integrative Anatomy and Evolutionary Biology* 295:1692-1697.
- Wen J, Sun D, Tan J, Young W (2015) A consistent, quantifiable, and graded rat lumbosacral spinal cord injury model. *J Neurotrauma* 32:875-892.
- Whishaw IQ, Faraji J, Kuntz JR, Agha BM, Metz GA, Mohajerani MH (2017) The syntactic organization of pasta-eating and the structure of reach movements in the head-fixed mouse. *Scientific reports* 7:1-14.
- Wu X, Zhang YP, Qu W, Shields LB, Shields CB, Xu X-M (2017) A tissue displacement-based contusive spinal cord injury model in mice. *JoVE (Journal of Visualized Experiments)*:e54988.

- Xu T, Yu X, Perlik AJ, Tobin WF, Zweig JA, Tennant K, Jones T, Zuo Y (2009) Rapid formation and selective stabilization of synapses for enduring motor memories. *Nature* 462:915-919.
- Zavvarian M-M, Hong J, Fehlings MG (2020) The Functional Role of Spinal Interneurons Following Traumatic Spinal Cord Injury. *Frontiers in Cellular Neuroscience* 14:127.
- Zholudeva LV, Qiang L, Marchenko V, Dougherty KJ, Sakiyama-Elbert SE, Lane MA (2018) The neuroplastic and therapeutic potential of spinal interneurons in the injured spinal cord. *Trends in neurosciences* 41:625-639.
- Zhu Y, Soderblom C, Trojanowsky M, Lee D-H, Lee JK (2015) Fibronectin matrix assembly after spinal cord injury. *Journal of neurotrauma* 32:1158-1167.

VITA

Chrystine Marie Gallegos was born in The Woodlands, Texas, in 1994, the daughter of Lynne Chrystine Ronemous and David G. Gallegos III. After completing her work at Cypress Woods High School, Cypress, Texas in 2013, she matriculated into Rice University in Houston, Texas. She received the degree of Bachelor of Arts with a major in Kinesiology – Sports Medicine and a minor in Biochemistry and Cell Biology with a Distinction in Research from Rice in May, 2017. For the following year, she worked as a research assistant in the Vivian L. Smith Department of Neurosurgery at The University of Texas Health Science Center at Houston. In August of 2018 she entered The University of Texas MD Anderson Cancer Center UTHealth Graduate School of Biomedical Sciences.

Permanent address:

1711 Old Spanish Trail #403

Houston, Texas 77054